INTERNATIONAL
HELLENIC
UNIVERSITY

Experimental and modelling study for the production of hydrogen via a novel intensified sorption enhanced chemical looping methane reforming process.

Aikaterini Giannakou

SID: 3302140013

SCHOOL OF SCIENCE & TECHNOLOGY

A thesis submitted for the degree of

Master of Science (MSc) in Energy Systems

DECEMBER 2015

THESSALONIKI – GREECE

INTERNATIONAL HELLENIC UNIVERSITY

Experimental and modelling study for the production of hydrogen via a novel intensified sorption enhanced chemical looping methane reforming process.

Aikaterini Giannakou

SID: 3302140013

Supervisor:	Dr. Eleni Herakleous
Supervising Committee Members:	Dr. Dimitrios Anastaselos
	Dr. Georgios Giannakidis

SCHOOL OF SCIENCE & TECHNOLOGY

A thesis submitted for the degree of

Master of Science (MSc) in Energy Systems

DECEMBER 2015

THESSALONIKI – GREECE

to my mom & my dad

Abstract

H_2 is considered as the energy vector of the future due to its clean combustion, resulting in almost no impact on the environment. However H_2 is a secondary energy carrier produced mainly through reforming of natural gas, which although a mature process remains very energy intensive. Sorption enhanced-chemical looping steam reforming is a novel process for efficient production of pure hydrogen, combining chemical looping steam reforming with in-situ CO_2 capture. In this process, the reformer contains, in addition to the sorbent, an oxygen transfer material (OTM). In the first step of this cyclic process, the oxide is reduced by CH_4 and serves as the reforming catalyst. The reaction proceeds under near autothermal conditions due to the heat released by the strongly exothermic carbonation reaction of the sorbent. In a second step, the saturated sorbent is regenerated with energy provided by the exothermic OTM re-oxidation.

This dissertation was written as a part of my MSc in Energy Systems at the International Hellenic University. The objective was to evaluate the effect of different operating conditions (temperature, steam/carbon ratio and OTM/sorbent ratio) on the performance of a previously developed optimized NiO-based OTM/catalyst (NiO/ZrO_2) and a CaO-based CO_2 sorbent ($CaO/CaZrO_3$) in the novel sorption enhanced steam methane reforming process combined with chemical looping concept. The experiments were carried out in a bench scale unit in Aristotle University of Thessaloniki, while a thermodynamic analysis of the process was performed using Aspen Plus® software.

Evaluation of the two solids indicated their suitability for the proposed process, with very stable performance under cyclic operation. The combined experiment demonstrated the feasibility and high potential of the novel process. Product concentrations in the outlet of the reformer closely followed the equilibrium at the different studied parameters. During the reforming stage, a very high H_2 concentration was achieved (>95%). During the regeneration stage, the highly exothermic Ni oxidation generates enough heat to increase the reactor's temperature from 650 to 800°C and supplies up to 45% of the heat required for the regeneration of the sorbent, for a NiO/CaO molar ratio of 0.8.

Acknowledgements

I am using this opportunity to express my appreciation for everyone who supported me throughout this dissertation. First of all, I would like to express my deepest gratitude to PhD Candidate Andy Antzara, for his guidance, patience, understanding and his excellent cooperation. His advices and his expertise were vital for the completion of my thesis. I would like also to thank my supervisor, Dr. Eleni Herakleous who let me experience this field of research. She has been a tremendous mentor for me during this master with her precious guidance and collaboration. I also cannot miss to thank Prof. Angeliki Lemonidou for hosting me for five months in her laboratory at Aristotle University of Thessaloniki with an excellent atmosphere for doing my thesis. Finally, I would also like to thank my family. They were always there supporting me, cheering me up and stood by me through the good times and bad. Thank you all.

Katerina Giannakou

11/12/2015

Contents

1 Introduction

This chapter constitutes an introduction on the importance of hydrogen, its uses and its production processes. In the beginning of the chapter the main routes for industrial hydrogen production are described, focusing on the dominant process, steam reforming of natural gas, while its installed capacity, industrial reformers and its disadvantages are presented. The next section of this chapter is focused on a novel process, the sorption enhanced chemical looping methane reforming, which is a combination of sorption enhanced reforming and chemical looping reforming. As this process is investigated in this thesis, the main advantages and disadvantages and its status will be presented. The chapter ends with the scope of this dissertation thesis.

1.1 Hydrogen – Importance, Uses and Production routes

The main efforts for a sustainable energy future focus on the reduction of carbon dioxide emissions and the improvement of urban air quality. Nowadays, climate change constitutes one of the greatest challenges facing our planet. The release and accumulation into the atmosphere of carbon dioxide (CO_2) and other gases is now far above pre-industrial levels and seems to be responsible for raising the world's average temperature through the greenhouse effect. It is evident that if carbon dioxide emissions from anthropogenic activities keep rising, the consequences will be disastrous for our global climate. As a consequence, there is need to move towards sustainable energy resources in order to secure energy supply and to create a new industrial and technological energy base [1, 2].

Hydrogen is considered as a key element, able to assist in issues of environmental emissions, sustainability and energy security. It is a clean fuel alternative which attracts a lot of interest in the last years. Hydrogen is not a primary energy source like coal or oil. It is considered as an "energy carrier", which must first be produced using energy from another source and then transported for future use [3]. It has the potential to pro-

vide energy in sections such as transportation, distributed heat and power generation and energy storage systems with little or no impact to the environment, both locally and globally [4].

It can be stored and used as a fuel in transportation, in distributed heat and power generation systems (fuel cells) and in internal combustion engines or turbines, with the only by-product being water. Hydrogen can also be used as storage medium for electricity generated from renewable resources, such as solar, wind, wave and tidal power via water electrolysis [1, 5].

Hydrogen can be obtained from various resources, as shown in Figure 1.1., including natural gas, coal and oil, biomass and water via electrolysis with renewable electricity produced from solar, wind, hydroelectric or geothermal energy. This variety of energy sources makes hydrogen a promising and important energy carrier. Moreover, hydrogen can be produced through a variety of process technologies, including thermal (natural gas reforming, biomass and coal gasification), electrolytic (water splitting) and photolytic processing (water splitting using sunlight via biological materials). However, hydrogen production has been dominated so far by fossil fuels, with the most significant technology being the steam methane reforming [6, 7].

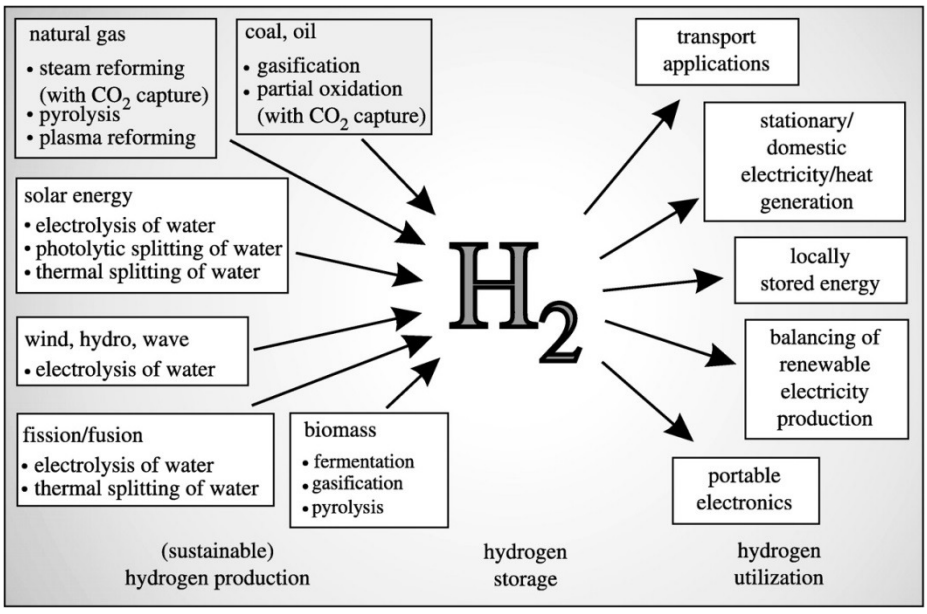

Figure 1.1: Hydrogen production methods through storage to different end-users [1].

1.2 Hydrogen from fossil fuels

Hydrogen can be produced from fossil fuels through three basic processes: (i) steam reforming (SR), (ii) partial oxidation (POX) and (iii) autothermal reforming (ATR).

1.2.1 Steam reforming (SR)

Steam Methane Reforming (SMR) is the dominant industrial process for hydrogen production today [8]. It is the most widespread and simultaneously the least expensive process [7, 9]. It has been used for several decades as an effective mean for converting hydrocarbons into hydrogen in the presence of steam. The heat efficiency of hydrogen production by the steam methane reforming process on an industrial scale is around 70–85% [10]. Typical capacities range from 1,000 to over 120,000 Nm³/h [11].

SMR is a multiple-step process (Fig. 1.2) and is characterized by harsh reaction conditions. More specifically, it is a catalytic process in which a reaction occurs between natural gas or other light hydrocarbons and steam. The product is a mixture of hydrogen, carbon monoxide, carbon dioxide and water [12].

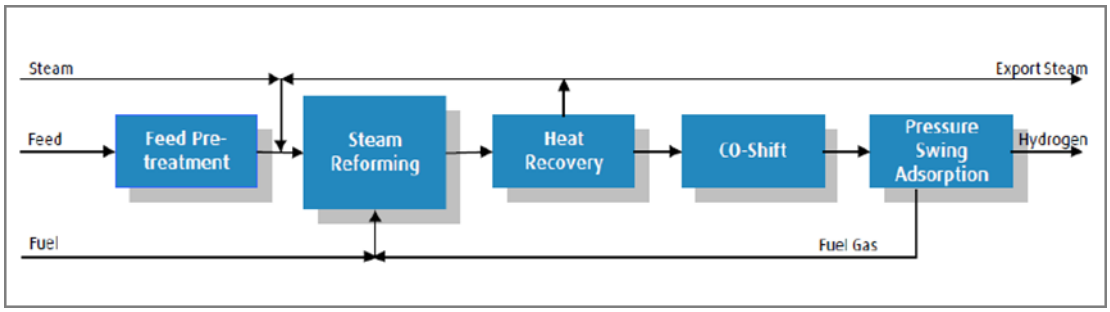

Figure 1.2: Schematic diagram of SMR process [13].

Firstly, methane catalytically reacts with steam into the reforming reactor to form hydrogen and carbon monoxide (Reaction 1.1) at a steam/carbon ratio of 1.8-4. The feed mixture is introduced into narrow chrome-nickel alloy reactor tubes containing pelleted catalysts as shown in Fig. 1.3. The reactor tubes are located inside a furnace which by heat transfer through the walls provides the necessary heat for the endothermic reaction [13]. The reforming reaction occurs at a temperature of 800-1000 °C and a pressure of 14-20 atm over a nickel-based catalyst [12]. Furthermore, it is a highly endothermic reaction, so a large amount of heat is provided by combustion of supplemental natural gas that is fed to the furnace.

$$CH_4 + H_2O \leftrightarrow CO + 3H_2,\ \Delta H^0_{298} = 206.2\ kJ\ /mol \qquad (1.1)$$

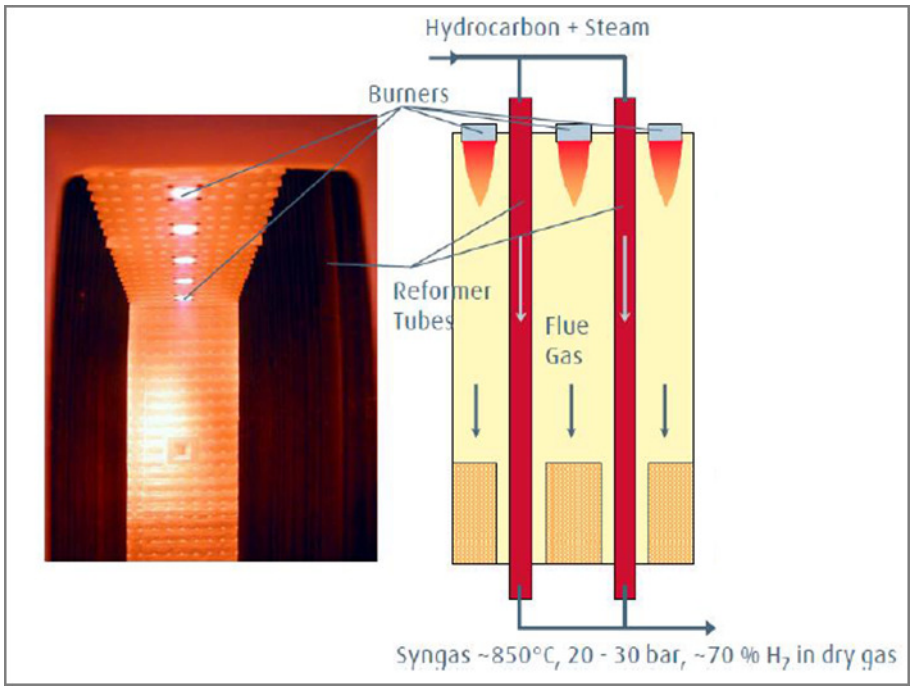

Figure 1.3: Steam reformer [14].

The reformate gas is then directed to a high (320-450°C) and a low temperature (200-250°C) Water Gas Shift reactors operating in series configuration, where the produced CO from the reformer reacts with steam over a catalyst via the water gas shift (WGS) reaction to form additional H_2 and CO_2 (Eq. (1.2)). The WGS reaction is slightly exothermic and is favored by low temperatures.

$$CO + H_2O \leftrightarrow CO_2 + H_2,\ \Delta H^0_{298} = -41.2\ kJ/mol \qquad (1.2)$$

After reforming and water gas shift, CO_2 and other impurities are removed from the gas stream using methanol as a washing solvent in a wash unit. Hydrogen is further purified usually in a pressure swing adsorption (PSA) unit.

Concluding, steam methane reforming even though mature, is a multi-step complex process with high energy demands. Almost 25% of natural gas feedstock is combusted as fuel to cover the energy demands of the endothermic steam reforming and reach the high reaction temperatures. In addition, it is a process with high CO_2 emissions and high investment cost for the construction of large furnaces [12].

1.2.2 Partial oxidation (POX)

Partial oxidation (POX) is a non-catalytic process, in which the raw material is gasified with oxygen (according to Reactions (1.3) and (1.4)) at temperatures between 1300 and 1500 ^{0}C and pressures between 3 and 8 MPa. The raw material can be primarily heavy hydrocarbons whose further utilization is difficult, methane and biogas.

$$CH_4 + O_2 \rightarrow CO + 2H_2 \quad (1.3)$$

$$CH_4 + 2O_2 \rightarrow CO_2 + 2H_2O \quad (1.4)$$

The process is completed with the conversion of carbon monoxide with steam into hydrogen and carbon dioxide (1.5).

$$CO + H_2O\,(g) \rightarrow CO_2 + H_2 \quad (1.5)$$

The products through partial oxidation contains CO, CO_2, H_2O, H_2, CH_4, hydrogen sulfide (H_2S) and carbon oxysulfide (COS). In comparison with the steam reforming, the processing temperature is very high, increasing the total installation cost due to the requirements of expensive materials that can withstand at the operating temperatures and the H_2/CO ratio is low [7, 15].

1.2.3 Autothermal reforming (ATR)

Autothermal reforming (ATR) combines the steam reforming (endothermic) with the partial oxidation (exothermic) reaction. In ATR process, oxygen is fed together with steam and methane in the reformer. Methane is partially oxidized by oxygen to carbon monoxide and hydrogen in the first part of the reactor providing the necessary heat for the endothermic steam reforming reaction. The upper part of an ATR reactor is similar to that of a partial oxidation reactor and it is followed by a catalytic steam reforming section (Fig. 1.4). In comparison with the steam methane reforming, ATR is a simpler process and there is no need for external heat [7, 15].

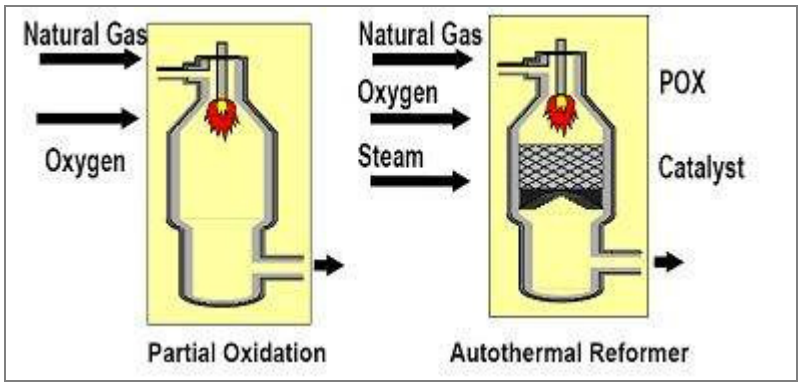

Figure 1.4: POX and ATR reactor [16].

The range of operation of a fuel reformer for hydrogen production can be seen in Figure 1.5. The selection of the conditions in which the reformer will operate depends on a specific target. A main target is the high hydrogen production with low carbon monoxide content. This is possible in steam reforming. However, steam reforming is a highly endothermic process that requires a high amount of energy provided in the reformer.

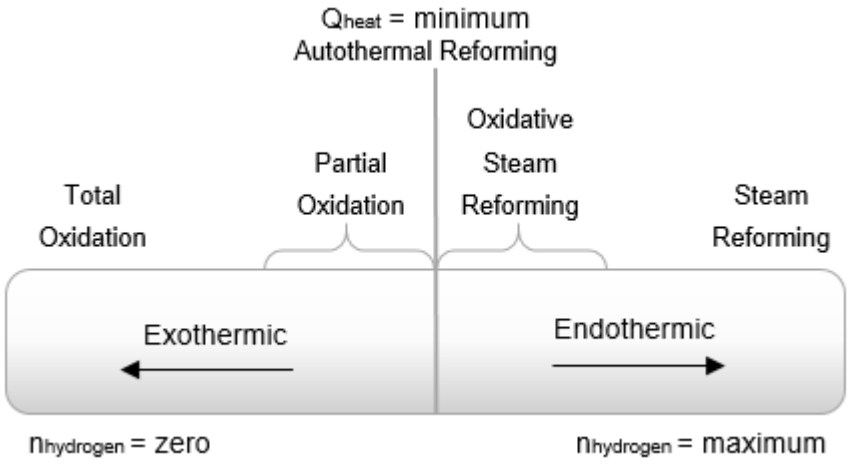

Figure 1.5: Operating conditions for SR, POX and ATR [7].

1.3 Hydrogen from renewables

Hydrogen can be also produced from renewable sources using processes other than reforming (Fig. 1.6). A brief description of the hydrogen production from biomass along with hydrogen production from water is described in this section.

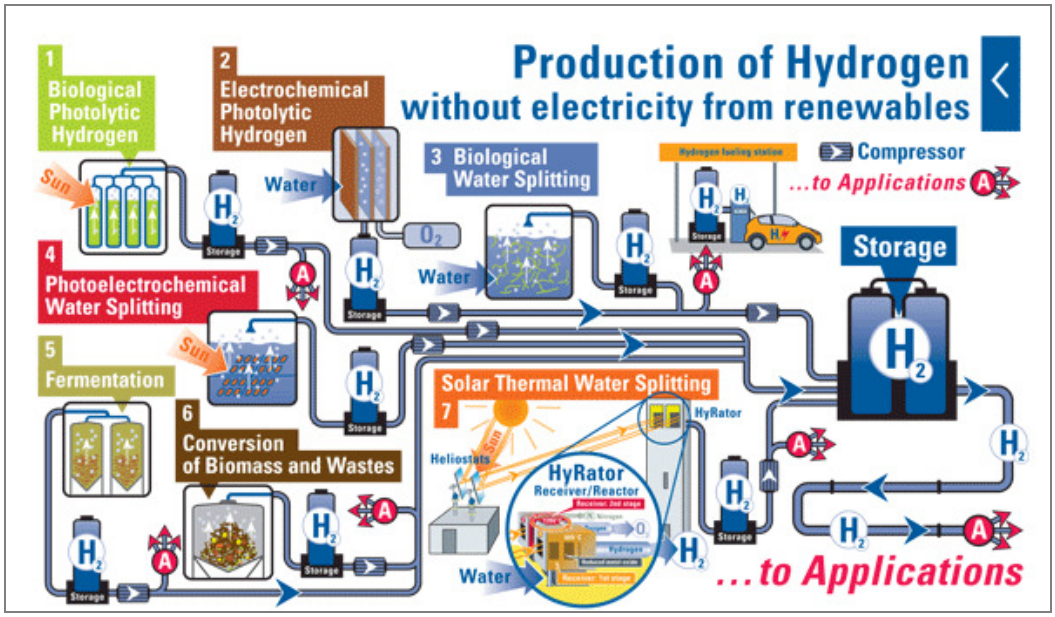

Figure 1.6: Hydrogen production from renewables [17].

1.3.1 Gasification

Gasification is a very mature technology and is commercially used in many processes (in the Fischer-Tropsch synthesis (liquid fuels) and in the synthesis of synthetic natural gas (SNG)). It is a commonly used technology with biomass or coal as a feedstock. There are many similarities between coal and biomass gasification as biomass can be considered as a very young coal. However there are also significant differences.

It is based on the partial oxidation of the feedstock material into a mixture of gases at high temperature greater than 800°C [18]. Addition of steam and/or oxygen in the process results in the production of syngas (H_2 and CO). Gasification can be performed with or without using a catalyst in a fixed-bed or a fluidized-bed reactor.

The gasification process is appropriate for biomass having moisture content less than 35%. In general, the yield of hydrogen is low from biomass due to the low hydrogen content in biomass (approximately 6% versus 25% for methane). Another problem of this technology is that provides significant amounts of tars (a complex mixture of higher aromatic hydrocarbons) in the product gas even operated in the 800–1000°C

range [19]. However, using biomass instead of coal in gasification overcomes the CO_2 emissions issue [7].

1.3.2 Pyrolysis

Another method of hydrogen production is pyrolysis. Biomass pyrolysis is one of the cheapest biomass conversion processes that can be economically applied on small scale. During pyrolysis, raw organic material is heated in inert atmosphere in the 500–900°C range [20]. Based on the temperature range, pyrolysis processes are divided into low (up to 500°C), medium (500–800°C), and high temperatures (over 800°C). The process takes place in the absence of oxygen and air. The reaction can be described by the following relationship: [21]

$$C_nH_m + \text{heat} \rightarrow n\,C + ½\,m\,H_2 \quad (1.6)$$

Since no water or air is present and no carbon oxides (CO or CO_2) are produced, there is no need for secondary reactors (like WGS). As a consequence, this process offers significant emissions reduction. It can be seen that biomass pyrolysis is a competitive method for renewable hydrogen production [7].

1.3.3 Electrolysis

Last but not least, electrolysis is a chemical process in which a direct current passes through two electrodes in a water solution and as a consequence the chemical bonds break into oxygen and hydrogen (Fig. 1.7):

$$\text{Cathode: } 2H_2O_{(l)} + 2e^- \rightarrow H_{2\,(g)} + 2OH^-_{(aq)} \quad (1.7)$$

$$\text{Anode: } 4OH^-_{(aq)} \rightarrow O_{2\,(g)} + 2H_2O_{(l)} + 4e^- \quad (1.8)$$

$$\text{Overall: } 2H_2O \rightarrow O_2 + 2H_2 \quad (1.9)$$

In practice, electrical energy is converted into chemical energy in the form of hydrogen, with oxygen as a byproduct. The reverse process occurs in a fuel cell.

Today, electrolysis is considered as the most promising process for renewable hydrogen production using indirect renewable energy resources. It produces only 4 % of world hydrogen production for applications that require very pure hydrogen such as electronics, pharmaceutical and food industries [22].

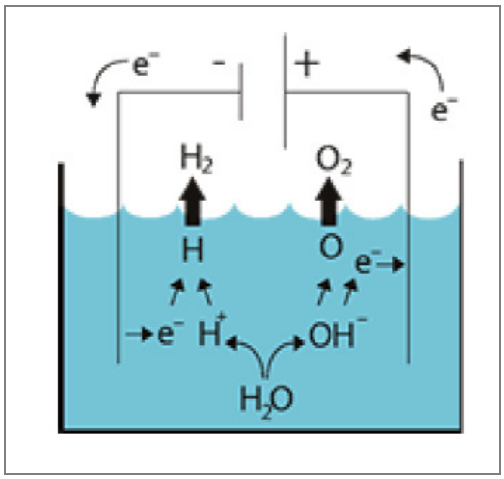

Figure 1.7: Electrolysis of water [23].

The process is ecological because no greenhouse gases are produced, and the oxygen formed has further industrial applications. Moreover, commercial production of hydrogen by electrolysis of water can achieve an efficiency of 75 %. However, in comparison with the methods described for the production of hydrogen from fossil fuels, electrolysis is a highly energy-demanding process [24]. Therefore water electrolysis makes sense only when the electricity used is surplus electricity from renewable energy sources.

The most mature technology is alkaline-based electrolysis while solid oxide electrolysis cells (SOEC) have been the least developed and the most electrically efficient technology [25]. Moreover, proton exchange membrane (PEM) electrolysis cells are more efficient than alkaline and do not have corrosion issues such as SOEC. However, they are more expensive than alkaline-based systems. Alkaline systems have the lowest capital cost and efficiency and thus they have the highest electrical energy cost [7, 26].

Taking everything into consideration, hydrogen can be produced from a variety of resources using a variety of process technologies. Significant development in hydrogen production processes from renewable resources such as biomass and water is being done. Biomass gasification constitutes one of the most mature technologies with minimal environmental impact. At the same time, electrolysis of water coupled with renewable energy is also one of the simplest technologies and can be considered as highly effective. However, currently, the most developed and used technology is the steam reforming of methane. One major drawback of steam methane reforming is its high emissions of CO_2 into the atmosphere. As a consequence, a tremendous amount of research is being carried out towards the sequestering of produced CO_2.

1.4 Intensifying natural gas reforming for high purity hydrogen production

Although conventional steam methane reforming is a mature technology which has been used for several decades, it still remains a very energy intensive process with high impact on the environment. It is evident that a new technology is required which will combine high efficiency with low emissions. At this direction, research efforts have been focused on two alternative reforming processes with lower energy demands, the Sorption Enhanced Reforming where the reforming reaction is combined with in-situ capture of the produced CO_2 and Chemical Looping Reforming that is an alternative to Autothermal Reforming process. The two novel processes that are at research level, are described thoroughly in the following paragraphs.

1.4.1 Sorption enhanced steam methane reforming (SE-SMR) using CO_2 sorbent

Sorption Enhanced Steam Methane Reforming (SE-SMR) is an emerging technology which combines the reforming reaction (H_2 production) with the selective separation of the produced CO_2 in a single reaction step, using a reforming catalyst mixed with a high temperature CaO-based CO_2 sorbent (Fig. 1.8) [27, 28].

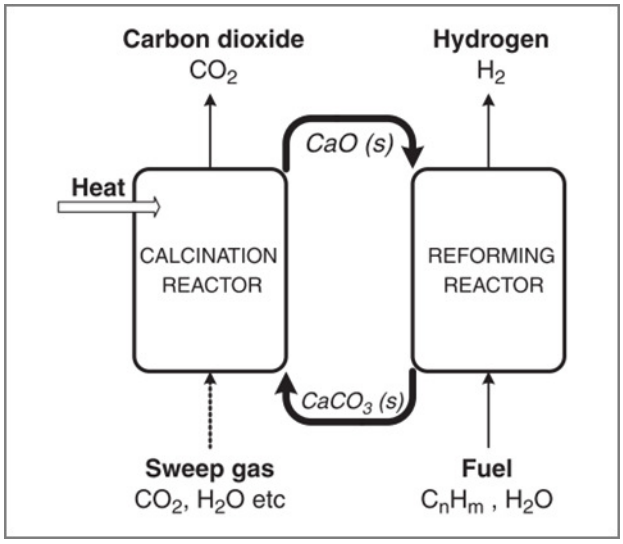

Figure 1.8: Schematic representation of SE-SMR with CaO as CO_2 sorbent [28].

More specifically, SE-SMR comprises the following three reactions:

1. steam methane reforming

$$CH_{4\,(g)} + H_2O_{\,(g)} \leftrightarrow CO_{\,(g)} + 3H_{2\,(g)},\ \Delta H_{298K} = 206\ kJ/mol \quad (1.10)$$

2. water-gas shift (WGS)

$$CO_{\,(g)} + H_2O_{\,(g)} \leftrightarrow CO_{2\,(g)} + H_{2\,(g)},\ \Delta H_{298K} = -\,41\ kJ/mol \quad (1.11)$$

3. In-situ CO_2 capture by the carbonation reaction of CaO

$$CO_{2\,(g)} + CaO_{\,(s)} \leftrightarrow CaCO_{3\,(s)},\ \Delta H_{298K} = -\,178\ kJ/mol \quad (1.12)$$

The overall reaction thus becomes [29]

$$CH_{4\,(g)} + 2H_2O_{\,(g)} + CaO_{\,(s)} \leftrightarrow 4H_{2\,(g)} + CaCO_{3\,(s)},\ \Delta H_{298K} = -\,13\ kJ/mol \quad (1.13)$$

The advantages of SE-SMR can be seen in thermodynamics. The combination of the endothermic reforming reaction with the exothermic sorption of CO_2 leads to an energetically well-balanced process with no heat demands. Moreover, the in-situ sorption of CO_2 shifts the equilibrium of the reforming and water gas shift reactions to the products site. As a consequence, the whole process can be performed at a much lower temperature than that of the conventional SMR process in a single step [29]. Moreover, the purity of the produced H_2 is much higher, thereby eliminating some of the H_2 purification step. However as the sorbent is gradually saturated in CO_2, the process requires a regeneration step in order to have continuous operation. Energy is required to regenerate the sorbent to its oxide form via the endothermic calcination reaction (reverse reaction 1.12) which occurs at higher temperatures in a second reactor (calciner) [28].

The equilibrium vapor pressure of CO_2 over CaO according to Eq. (1.12) can be calculated as a function of temperature in which the carbonation and calcination reactions occur. As illustrated in Fig. 1.9, partial pressures of CO_2 greater than the equilibrium partial pressure at a given temperature will favor carbonation, while those lower than the equilibrium will favor calcination. More specifically, during the exothermic carbonation reaction, as temperature increases, the minimum required partial pressure of carbon dioxide also increases in order sorption of CO_2 to be carried out. Moreover, at low temperatures reforming reaction of methane is not favored, resulting in lower partial pressure of carbon dioxide. As a result an intermediate temperature in the range of 600-700°C is usually chosen in order to favor both the endothermic methane reforming and the exothermic CaO carbonation and achieve high conversions. After sorbent's sat-

uration a higher temperature is required in order for the reverse carbonation reaction (calcination) to take place. Thus, by increasing temperature, the minimum partial pressure of carbon dioxide required for carbonation of CaO also increases, leading to decomposition of the $CaCO_3$ [27, 30, 33].

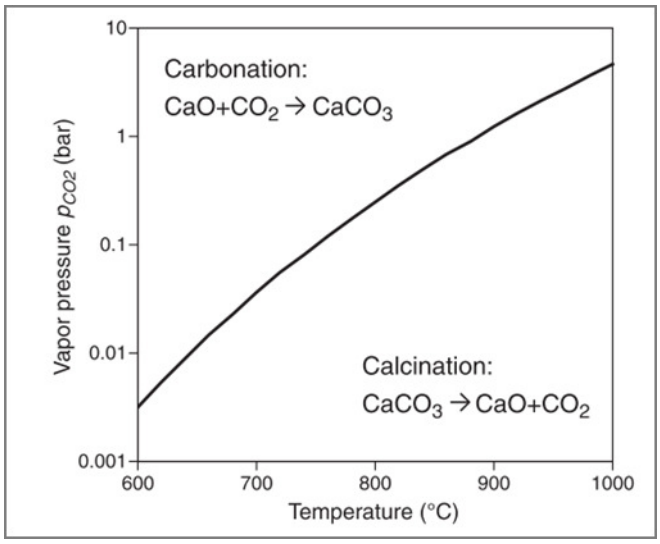

Figure 1.9: Vapor pressure of CO_2 as a function of temperature [28].

Concluding, SE-SMR conduces to:

i. higher efficiency in high purity hydrogen production;

ii. elimination of the WGS (water gas shift) reactor and further purification;

iii. save energy of 20 – 25 % compared to SMR;

iv. reduction of the operating temperature compared to SMR which may reduce catalyst sintering;

v. replace high alloy steels required in the reactor with less expensive wall materials;

vi. production of a pure CO_2 stream ready for sequestration or other application [27].

Selection of the proper solid sorbent constitutes the most important part of the SESMR process. An appropriate sorbent for SE-SMR should have good stability and maintain its activity in cyclic sorption-desorption operation (reaction-regeneration cycles), preventing thermal sintering and shocking. In addition, it should have low temperature interval between carbonation and calcination and low cost [12, 27, 31].

CaO-based materials are considered as efficient CO_2 sorbents because of their appropriate kinetics and moderate sorption capacity. Calcines of natural limestones can be used as high-temperature sorbents and so excess heat can be recovered to provide additional energy to capture CO_2. In addition, limestones are low-cost, easy to find and characterized by high adsorption ability. However, it is well known that the decay of their carbonation conversion through multiple carbonation/ calcination cycles can limit their applicability. Loss in sorbent reactivity can be caused by material sintering and reduction of the reactive surface area during the high temperature calcination stage. Nevertheless, addition of supports or incorporation of active CaO into inert solid matrix is a very promising method to prevent or delay them from sintering at high temperature. Compared to pure CaO, most of the synthetic CaO-based sorbents show much higher CO_2 capture capability and stability during many carbonation-calcination cycles [32-37].

1.4.2 Chemical Looping Reforming (CL-R)

Chemical looping reforming is a novel technology that uses a solid oxygen carrier such as a metal oxide to transfer oxygen from air to the fuel avoiding the direct contact between them. The oxidation of the fuel occurs via the cyclic reduction and oxidation of the solid oxygen carrier. During this process, the air to fuel ratio is low thus preventing from complete oxidation of the fuel to CO_2 and H_2O [38].

The concept in CL-R is to partially oxidize hydrocarbons into two distinct steps as shown in Fig. 1.10. In the first step, the fuel (CH_4) is fed to the reforming reactor, where it is oxidized via a solid oxygen carrier. Part of the fuel may be completely oxidized to CO_2 and H_2O, but most of it should be partially oxidized to CO and H_2.

$$CH_{4\,(g)} + MeO_{\,(s)} \leftrightarrow CO_{\,(g)} + 2H_{2\,(g)} + Me_{\,(s)},\ \Delta H > 0 \qquad (1.14)$$

The reduced oxygen carrier is taken to the air reactor, where it is oxidized to its initial state with O_2 provided from air.

$$Me_{\,(s)} + 1/2O_{2\,(g)} \rightarrow MeO_{\,(s)},\ \Delta H < 0 \qquad (1.15)$$

The overall reaction thus becomes

$$CH_{4\,(g)} + 1/2O_{2\,(g)} \rightarrow CO_{\,(g)} + 2H_{2\,(g)},\ \Delta H < 0 \qquad (1.16)$$

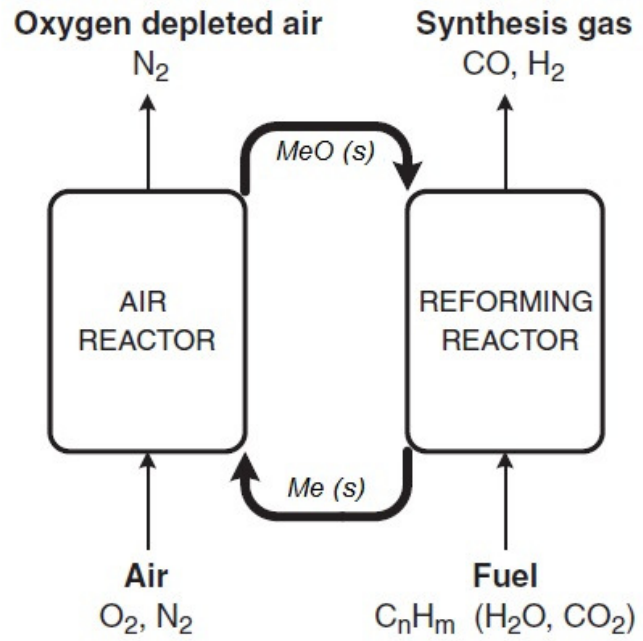

Figure 1.10: Schematic representation of CL-R with MeO as oxygen carrier [28].

The oxidation reaction of the oxide carrier is very exothermic, whereas the reduction reaction is endothermic. So, the required heat is provided by the circulating solids exiting from the air reactor at higher temperature. Therefore, the heat generated in the air reactor is high enough to carry out the heat balance of the system.

The major advantage of this process is that the required heat for converting CH_4 to H_2 is supplied without mixing of air with carbon containing fuel gases or without using part of the H_2 produced in the process. The products are not diluted with nitrogen from air and the need for gas separation is eliminated [38].

A suitable oxygen carrier for a CL-R process should fulfill the following properties:

i. high reactivity through cycles;

ii. high resistance to attrition;

iii. Selective in partial oxidation reaction in order to completely convert the fuel to CO and H_2;

iv. negligible carbon deposition;

v. good properties for fluidization (no presence of agglomeration);

vi. easy preparation

Although, various metal oxides have been proposed in literature as possible oxygen carriers, such as CuO, NiO, Fe_2O_3 and CoO [39-42], NiO would be an excellent choice for CL-R. NiO has proven to fulfill all the properties outlined above. In addition, once it is reduced to metallic Ni, it also has strong catalytic properties, facilitating a number of reactions such as steam reforming and water–gas shift [28].

1.4.3 *Sorption enhanced chemical looping steam methane reforming (SE-CL-SMR)*

Sorption enhanced chemical looping steam methane reforming (SE-CL-SMR) is a novel method for conversion of hydrocarbons to hydrogen, integrating sorption enhanced reforming with chemical looping reforming. This combined process takes advantage of both sets of chemical loops mentioned above producing H_2 with inherent CO_2 capture without need for water-gas shift reactors and gas separation operations and without need for external heat supply.

In sorption enhanced chemical-looping steam methane reforming, reforming reactor contains a suitable CO_2 sorbent such as CaO together with a solid oxygen carrier such as NiO as bed materials. The oxygen transfer material is reduced by methane (Reactions (1.18) and (1.19)) and catalyzes the steam reforming reaction (Reaction (1.17)). The produced CO is shifted to CO_2 via the water gas shift reaction, facilitated by the capture of the produced CO_2 via the carbonation reaction of CaO (Reactions 1.20 and 1.21 respectively). The overall reaction in the reforming reactor is nearly energy neutral, as most of the energy required for the reforming reaction is covered in-situ from the carbonation reaction of calcium oxide.

$$CH_{4\,(g)} + H_2O_{\,(g)} \leftrightarrow CO_{\,(g)} + 3H_{2\,(g)},\ \Delta H_{298\,K} = 206\ kJ/mol \quad (1.17)$$

$$CH_{4\,(g)} + 4NiO_{\,(s)} \leftrightarrow CO_{2\,(g)} + 2H_2O_{\,(g)} + 4Ni_{\,(s)},\ \Delta H_{298\,K} = 123\ kJ/mol \quad (1.18)$$

$$CH_{4\,(g)} + NiO_{\,(s)} \leftrightarrow CO_{\,(g)} + 2H_{2\,(g)} + Ni_{\,(s)},\ \Delta H_{298\,K} = 203\ kJ/mol \quad (1.19)$$

$$CO_{\,(g)} + H_2O_{\,(g)} \leftrightarrow CO_{2\,(g)} + H_{2\,(s)},\ \Delta H_{298\,K} = -41\ kJ/mol \quad (1.20)$$

$$CO_{2\,(g)} + CaO_{\,(s)} \leftrightarrow CaCO_{3\,(s)},\ \Delta H_{298\,K} = -179\ kJ/mol \quad (1.21)$$

After sorbent's saturation, the solids are transferred in a second reactor (regenerator), where both calcination of the sorbent and re-oxidation of the OTM take place in a single step. The reduced oxygen carrier is re-oxidized in the presence of a suitable oxidant such as pure O_2 or air according to the following reactions.

$$Ni_{(s)} + 1/2O_{2(g)} \rightarrow NiO_{(s)},\ \Delta H_{298\,K} = -240\ kJ/mol \quad (1.22)$$

$$Ni_{(s)} + ½\,(O_{2(g)} + 3.76N_{2(g)}) \rightarrow NiO_{(s)} + 1.88N_{2(g)},\ \Delta H_{298\,K} = -240\ kJ/mol \quad (1.23)$$

In the case that pure oxygen is used as oxidant, the only product leaving the regenerator is CO_2 produced from calcination of the saturated sorbent since oxygen is totally consumed in Reaction (1.22). This reaction is strongly exothermic thus providing the energy required for the regeneration of the sorbent, which is reused in the reforming reactor.

When air is used for the re-oxidation, the CO_2 leaving the reactor is diluted in N_2. As a result an additional separation step will be required that will have an energetic and economic impact (cost) on the process. The regeneration cycle will take place in two reactors. In the first one Ni will be oxidized to NiO with air while in the second one the sorbent will be regenerated in the presence of H_2O or CO_2 [43].

1.5 Scope of dissertation

Global production of hydrogen has so far been dominated by fossil fuels, with the most important technology being the steam reforming of natural gas, an energy demanding process with high environmental impact. Chemical looping reforming and sorption enhanced steam reforming are two innovative technologies aiming to develop an energy autonomous system for hydrogen production using an oxygen carrier or a hydrogen production system with in situ carbon dioxide capture in a single step using a CO_2 sorbent respectively. The integration of both methods leads to a promising cyclic process, the sorption enhanced chemical looping steam reforming, which produces a high purity hydrogen stream in a single step with in situ separation of carbon dioxide in a ready for sequestration stream. The reaction in the reformer operates under nearly autothermal conditions due to the heat released by the exothermic carbonation reaction of the CO_2 sorbent, while in a second step, the regeneration of the saturated sorbent is driven by the exothermic OTM reoxidation. The key for the successful commercialization of this novel process is the development of a CO_2 sorbent material and a solid oxygen carrier-reforming catalyst with good stability in reaction-regeneration cycles.

The scope of this dissertation was to experimentally assess the effect of operating conditions such as reactor temperature, steam/carbon ratio and OTM/sorbent ratio on the performance of a previously developed optimized OTM and sorbent solid materials in sorption enhanced chemical looping steam methane reforming. A thermodynamic and experimental analysis was performed to determine the optimum operating conditions for the sorption enhanced chemical looping methane reforming. The thermodynamic analysis was carried out using the simulation software Aspen Plus® in order to demonstrate the operation of the reforming reactor. On the other hand, the experiments were conducted at atmospheric pressure in a laboratory flow unit equipped with a tubular fixed bed reactor in the Department of Chemical Engineering at the Aristotle University of Thessaloniki. Finally, the main findings of the experimental study were compared to those revealed from the simulation study.

2 Process Simulation Study

Chapter 2 is dedicated to the simulation of sorption enhanced chemical looping steam methane reforming using the simulation software Aspen Plus®. A thermodynamic analysis was performed to determine the optimum operating conditions for this novel process. Simulation of the conventional reforming process under the same conditions was conducted for comparison reasons. In the first part, the followed methodology is thoroughly described and the flow diagrams of conventional SMR and the proposed process are presented. The effect of different operating conditions such as temperature, S/C ratio and OTM/sorbent ratio on the reactor's product concentration and H_2 yield are investigated.

2.1 Simulation methodology

Conventional steam methane reforming process and sorption enhanced chemical–looping steam methane reforming process were simulated, with the aim of finding appropriate operating conditions for the production of hydrogen. The simulations were carried out by Aspen Plus software, performing basic equilibrium calculations in order to estimate the effect of different parameters (temperature, S/C ratio, NiO/CaO ratio).

The most commonly used expression for the equilibrium state is Gibbs free energy. The minimization of total Gibbs free energy is an appropriate path method for the calculation of the equilibrium compositions of any reactant at specific temperature and pressure. By applying this method, the reactions are not specified by the user, but the reactants, products and temperature are [44].

RGibbs reactor calculates the equilibrium composition, based in the minimum Gibbs free energy according with input streams and process conditions (temperature and pressure). It is a flexible model that allows multiple phases including solid phases. Furthermore, it operates non-adiabatically so heat is removed or provided to each reactor in order to put through constant conditions in every step of a process [43].

In addition, SSplit model was used as a cyclone separator that performs the separation of mixed streams that come out of the reactors into two streams, solid and gaseous. It is an ideal model so it is assumed that it operates at 100 % efficiency.

Physical properties were described using PENG–ROB, Aspen Peng – Robinson's equation, which is suitable for non – polar or mildly polar components and mixtures such as hydrocarbons and light gases (e.g. carbon oxides, hydrogen etc.).

The following were assumed during the simulation of the two processes (conventional steam methane reforming and sorption enhanced chemical-looping steam methane reforming):

- Natural gas consists only of methane.
- The species that are present in the balance under the investigated conditions are: CH_4, H_2O, H_2, CO_2, CO and O_2.
- In addition to the above components, in the case of SE-CL-SMR process, CaO, $CaCO_3$, Ni and NiO were assumed to be also present in the calculation of the reactor's equilibrium.
- Carbon deposition is negligible.
- Pressure is constant at 1 atm throughout the process and reference temperature is 25 °C.
- The inlet streams are preheated by heat exchange with the hot product streams. The minimum temperature difference between the outlet temperatures of the hot and the cold stream of a heat exchanger is 20 °C.
- Both the CaO sorbent and the NiO oxygen carrier are fully regenerated/re-oxidized and do not exhibit any change in their reactivity during multiple sorption/desorption-oxidation/reduction cycles respectively.
- The residence time inside the reactor is enough in order all reactions reach equilibrium.

Sensitivity analysis was performed for a range of temperatures, H_2O/CH_4 (S/C) ratios and NiO/CaO (OTM/sorbent) ratios. The type and range of investigated parameters for the reforming/reduction/carbonation cycles are tabulated in Table 2.1. The parametric study of the reformer was based on the effect of the above parameters in H_2, CH_4, CO and CO_2 concentrations in the outlet of the reactor, as well as in CH_4 conversion and H_2 yield of each process.

Table 2.1: Range of investigated parameters.

Temperature [°C]	H_2O/CH_4 (S/C) ratio	NiO/CaO (OTM/sorbent) ratio
600 – 800	2 – 4	0 – 1

H_2, CH_4, CO and CO_2 concentrations are defined as the amount of each component produced (H_2, CH_4, CO or CO_2-moles) divided by the total moles of the gaseous outlet stream of the reformer (dry basis):

$$\%\, X\ concentration = \frac{n_{X,produced}}{n_{X,out}} \cdot 100 \quad (2.1)$$

where X: H_2, CH_4, CO, CO_2

CH_4 conversion is defined as the number of moles of CH_4 that reacted (moles in inlet minus the moles in the outlet) divided by the moles of CH_4 in the feed stream of the reformer:

$$\%\, CH_4\ conversion = \frac{(n_{CH_4,in} - n_{CH_4,out})}{n_{CH_4,in}} \times 100 \quad (2.2)$$

H_2 yield is defined as the amount of produced H_2 (moles) divided by the stoichiometric amount of produced H_2 by the reforming reaction, which is 4 moles of H_2 per mol of CH_4 [43]:

$$\%\, H_2\ yield = \frac{n_{H_2,out}}{n_{H_2,stoich}} \cdot 100 \quad (2.3)$$

2.2 Process flow diagram

2.2.1 Conventional Steam Methane Reforming (SMR)

In the case of conventional SMR, it was considered that only the methane reforming reaction (Eq. 2.4) and the water gas shift reaction (Eq. 2.5) take place. At the corresponding industrial process, there are also a high and a low WGS reactor for further conversion of CO to CO_2 and a stage for the further purification of hydrogen. However, in our case, only the reformer was simulated in order to directly compare its results with that obtained from the experimental process.

$CH_4 + H_2O \leftrightarrow CO + 3H_2$, $\Delta H_{298\ K} = 206$ kJ /mol (2.4)

$CO + H_2O \leftrightarrow CO_2 + H_2$, $\Delta H_{298\ K} = -41$ kJ /mol (2.5)

Conventional steam methane reforming process was simulated using the Aspen plus Software. The flowchart of the process was designed using the Microsoft Office Visio Software and is presented in Scheme 2.1.

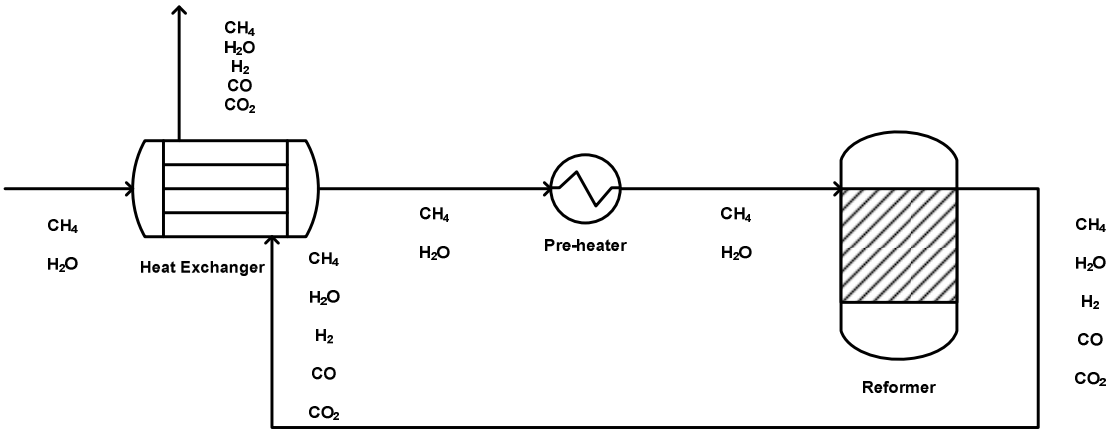

Scheme 2.1: Simulation flow diagram of the conventional steam methane reforming process.

As it is observed from the above flowchart, the system consists of a reformer, more specifically an RGibbs reactor as well as a heat exchanger and a pre-heater. The reactant stream, methane and steam is preheated in a heat exchanger utilizing the heat load of the hot product stream, in order to reduce the thermal requirements of the process and then it is fed into to a pre-heater where the feed stream is preheated to the reaction temperature prior entering the reforming reactor. The reactor is assumed to operate non-adiabatically, under isothermal conditions and atmospheric pressure. The product stream contains hydrogen as a major product, some fractions of methane, unreacted steam, carbon dioxide and carbon monoxide.

During the simulation of conventional SMR process, a sensitivity analysis was performed. The reforming temperature was varied from 600 °C to 800 °C in the analysis as well as the (S/C) ratio was varied from 2 to 4 in order to determine the effect of these parameters on the process. The results of these simulations will be presented in the next section 2.3.

2.2.2 Sorption Enhanced Chemical-Looping Steam Methane Reforming (SE-CL-SMR)

In sorption enhanced chemical-looping steam methane reforming process, the reformer contains a CaO-based CO_2 sorbent and an OTM (NiO). In the presence of CaO, the produced CO_2 is in-situ separated from the products by the carbonation reaction of CaO (Eq. 2.6), driving the equilibrium of reactions 2.4 and 2.5 to the right and leading to higher methane conversions and hydrogen yields.

$$CO_{2\,(g)} + CaO_{\,(s)} \leftrightarrow CaCO_{3\,(s)},\ \Delta H_{298\,K} = -179\ kJ/mol \qquad (2.6)$$

In addition to reaction 2.4-2.6, part of methane and the produced reformate gas is consumed for NiO reduction, according to the following reactions:

$$CH_{4\,(g)} + H_2O_{\,(g)} \leftrightarrow CO_{\,(g)} + 3H_{2\,(g)},\ \Delta H_{298\,K} = 206\ kJ/mol \qquad (2.7)$$

$$CH_{4\,(g)} + 4NiO_{\,(s)} \leftrightarrow CO_{2\,(g)} + 2H_2O_{\,(g)} + 4Ni_{\,(s)},\ \Delta H_{298\,K} = 123\ kJ/mol \qquad (2.8)$$

$$CH_{4\,(g)} + NiO_{\,(s)} \leftrightarrow CO_{\,(g)} + 2H_{2\,(g)} + Ni_{\,(s)},\ \Delta H_{298\,K} = 203\ kJ/mol \qquad (2.9)$$

$$CO_{\,(g)} + H_2O_{\,(g)} \leftrightarrow CO_{2\,(g)} + H_{2\,(s)},\ \Delta H_{298\,K} = -41\ kJ/mol \qquad (2.10)$$

When the sorbent is fully saturated with CO_2, it is then fully regenerated at higher temperature (reversed 2.6) at the regenerator, where simultaneously the re-oxidation of the reduced OTM by a suitable oxidant such as pure O_2 occurs, according to the following reaction:

$$Ni_{\,(s)} + 1/2O_{2\,(g)} \rightarrow NiO_{\,(s)},\ \Delta H_{298\,K} = -240\ kJ/mol \qquad (2.11)$$

SE – CL – SMR process was simulated using the Aspen plus Software. The flowchart of the process was designed using the Microsoft Office Visio Software and is presented in Scheme 2.2. The simulated system consists of a reforming reactor, a reactor for the regeneration of the sorbent and the re–oxidation of the OTM, two cyclone separators, one mixer, as wells as two heat exchangers and two preheaters.

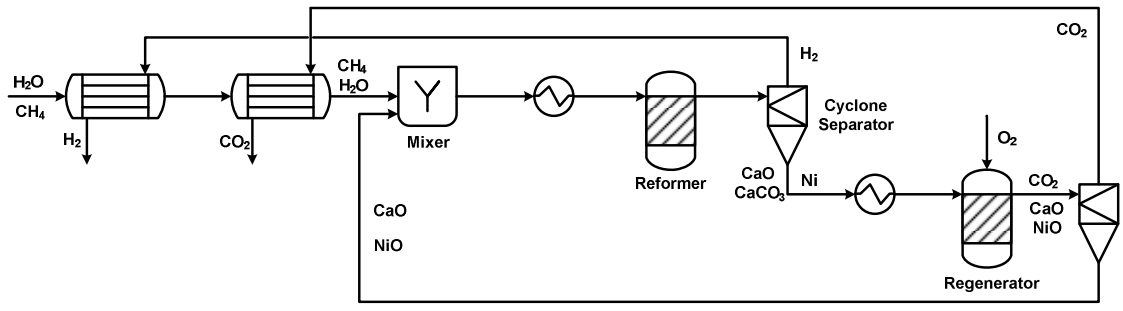

Scheme 2.2: Simulation flow diagram of the SE – CL – SMR process.

Methane and water (reactant stream), at reference temperature and at atmospheric pressure, is preheated via heat exchangers utilizing the heat of the produced H_2 from the reformer and the produced CO_2 from the regenerator. Then, methane and steam are fed into the reformer under isothermal conditions at atmospheric pressure. The major product is hydrogen, but in the product stream there are also unreacted CH_4 and H_2O, CO, CO_2, CaO, $CaCO_3$ and Ni. All of the products are transported to a cyclone where Ni, CaO and $CaCO_3$ solids are separated from the gases. The hydrogen-rich gas stream passes through the heat exchangers and exchanges heat with the fresh reactant stream, CH_4 and H_2O, which is pre-heated.

The separated Ni, CaO and $CaCO_3$ solids are transferred to the regenerator, which operates at 820 °C and 1 atm. Here, $CaCO_3$ is calcined into CaO releasing CO_2 in the presence of a suitable sweep gas (steam). Simultaneously, Ni reacts with O_2 under adiabatic conditions, forming NiO. The gas and solid stream is fed to the second cyclone where the NiO and CaO are separated from the CO_2. The CO_2-rich gas stream then passes through a heat exchanger exchanging heat with the reactant stream and both of them are led to the reformer. The solids are fed to the reformer after mixing with the reactants.

2.3 Simulation results

2.3.1 Effect of temperature

Temperature constitutes one of the most important parameters that could regulate the equilibrium in a reforming reactor due to the fact that simultaneous endothermic and exothermic reactions occur during its operation. For this reason, a sensitivity analysis was performed for a range of temperatures to find the optimal one for the operation of a reforming reactor. Figure 2.1 illustrates the effect of temperature on product concentrations (% H_2, CH_4, CO_2 and CO in dry basis) in the outlet of the reformer for the conventional SMR and SE-CL-SMR process.

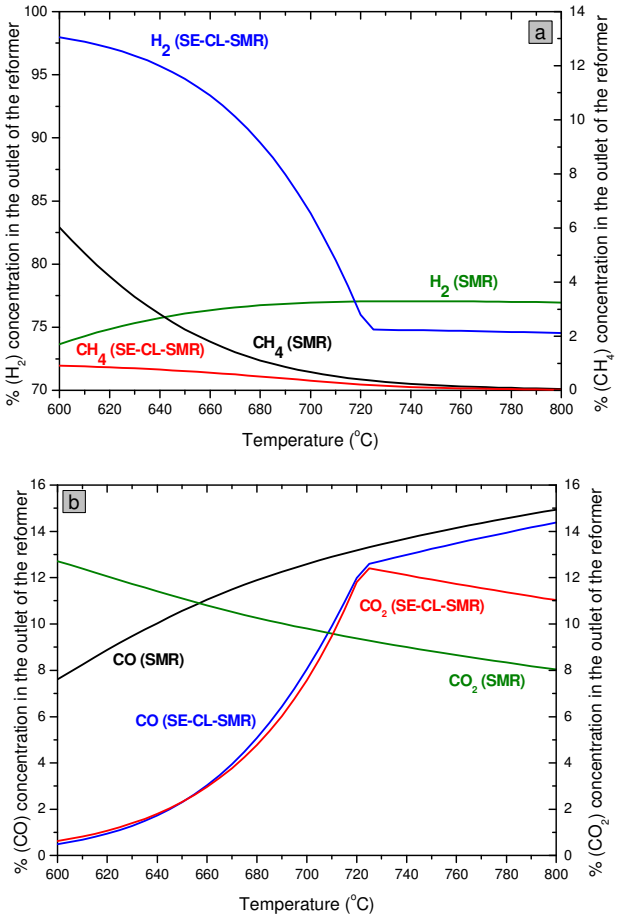

Figure 2.1: Product concentration in the outlet of the reformer (a: H_2 and CH_4 concentrations, b: CO and CO_2 concentrations) for the conventional SMR and SE-CL-SMR process (T=600-800°C, S/C ratio=3, CaO/C=1, NiO/CaO=0.5).

In conventional SMR process, an increase in the reformer's temperature greatly decreases methane concentration while increases hydrogen concentration. This is an expected result since the endothermic reforming reaction is favored by high temperatures, shifting to the right. However, this trend of increasing hydrogen with increasing temperature approaches a limit for temperature over 650 °C (Fig. 2.1a).

On the other hand, in SE-CL-SMR process, the presence of CO_2 sorbent results in higher concentrations of hydrogen even at temperatures below 650 °C. This is a result of the exothermic carbonation reaction, which shifts the reactions to the right at lower temperatures, promoting the formation of hydrogen. Moreover, the presence of the NiO oxygen carrier in the SE-CL-SMR leads to even lower methane concentration than that in the SMR due to partial and total oxidation of part of methane by oxygen provided from NiO reduction.

Regarding CO and CO_2 concentrations, the addition of CO_2 sorbent shifts the reforming and WGS reactions to the right resulting in very low CO and CO_2 concentrations in the outlet of the reformer. As temperature increases, the positive effect of CO_2 capture declines. At temperatures higher than 720 °C, the sorption of carbon dioxide is no longer possible due to the fact that partial pressure of CO_2 in the system is lower than its equilibrium partial pressure which favors $CaCO_3$ decomposition to CaO and CO_2. As a consequence, at temperatures above 720 °C the sorption enhanced process degenerates into conventional steam reforming.

Concluding, for temperatures above 650 °C, the sorption capacity of the sorbent reduces gradually thereby reducing both methane conversion and hydrogen yield making the process less attractive. As a result, the optimum reactor operating conditions at 1 atm approximates to be at a temperature range between 600 and 650 °C, leading to an approximate hydrogen concentration of 95 %.

2.3.2 Effect of (S/C) ratio

As steam is a reactant in both reforming and water gas shift reaction, a change in steam to carbon (S/C) ratio can affect the equilibrium of these two reactions and generally of SMR and SE-CL-SMR processes. For this reason, a sensitivity analysis was performed for a range of S/C ratios to find the optimal one for the reforming reactor. Figure 2.2 presents the outlet concentrations (% H_2, CH_4, CO_2 and CO) of the reformer as a function of steam to carbon ratio for conventional SMR and SE-CL-SMR processes.

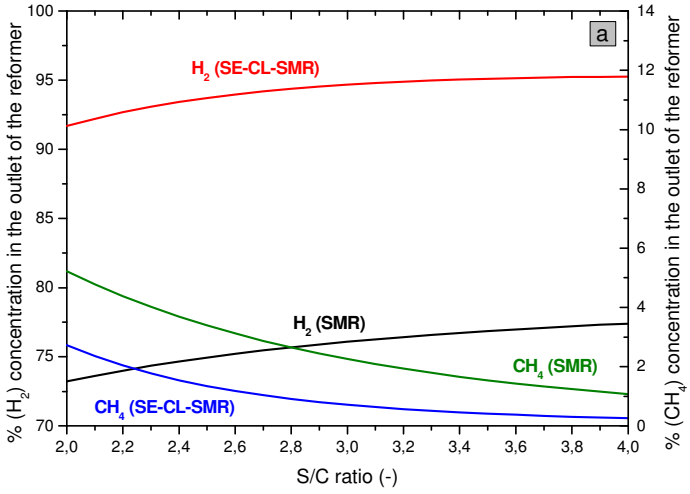

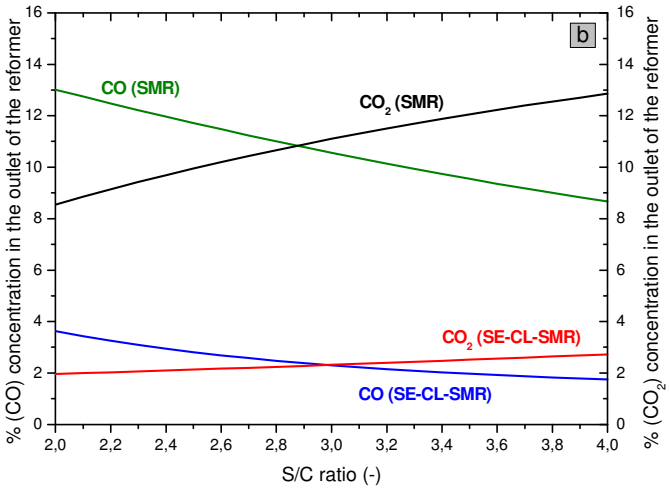

Figure 2.2: Product concentration in the outlet of the reformer (a: H_2 and CH_4 concentrations, b: CO and CO_2 concentrations) for the conventional SMR and SE-CL-SMR process (T=650°C, S/C ratio=2-4, CaO/C=1, NiO/CaO=0.5).

S/C ratio has a significant effect on the processes as an increase drives the equilibrium of both conventional SMR and SE-CL-SMR in the same direction. By increasing the amount of steam in the feed stream, the equilibrium of the reforming and water gas shift reaction is shifted to the products side, resulting in higher production of hydrogen, as expected.

Furthermore, the shift of the equilibrium of the water gas shift reaction to the right increases the production of CO_2 and the consumption of CO. At the same time, the partial pressure of CO_2 increases favoring the carbonation reaction of CaO, which leads to the production of a hydrogen with higher purity. This effect is more pronounced at S/C ratios lower than three and seems to level off at higher values.

However, the increase of S/C ratio requires a considerable amount of heat in order to generate high pressure steam for the reaction, greatly decreasing the efficiency of the process. In addition, for values of the ratio S / C of greater than 3 is not observed any substantial change in the efficiency of processes. Therefore an intermediate S/C ratio in the range of 3 is generally used.

2.3.3 Effect of NiO/CaO ratio

The ratio of NiO/CaO plays an important role in SE-CL-SMR process as part of the required heat for the calcination of $CaCO_3$ can be provided in-situ by the reoxidation of Ni reducing the overall thermal requirements of the SE-CL-SMR process. Figure 2.3 illustrates the effect of NiO/CaO ratio on the equilibrium product concentrations (% H_2, CH_4, CO_2 and CO in dry basis) in the outlet of the reformer for the SE-CL-SMR process.

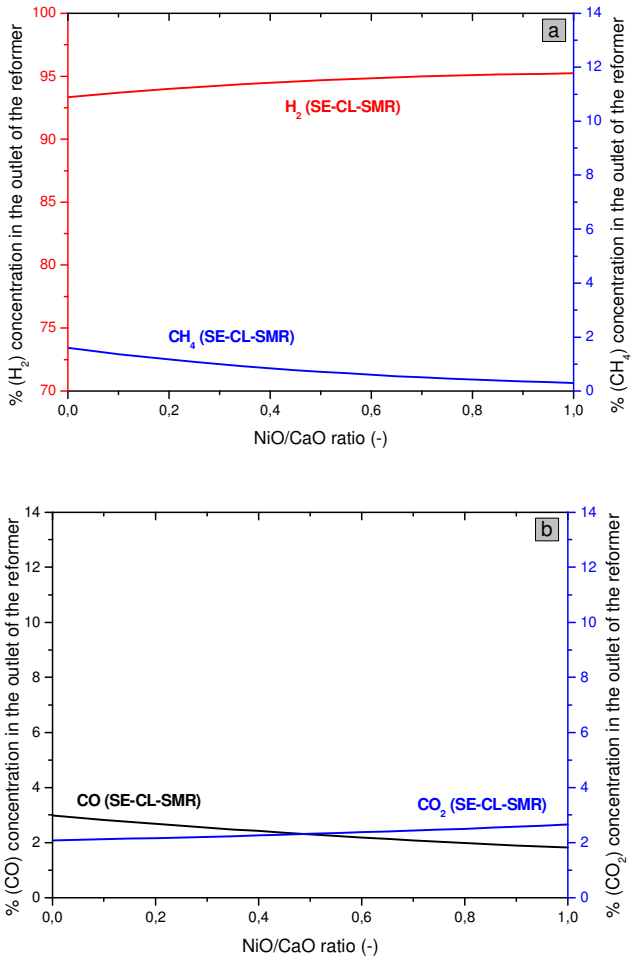

Figure 2.3: Product concentration in the outlet of the reformer (A: H_2 and CH_4 concentrations, B: CO and CO_2 concentrations) for the conventional SMR and SE-CL-SMR process (T = 650 °C, S/C ratio = 3, CaO/C = 1, NiO/CaO = 0-1).

Based on the above Figure 2.3a, H_2 concentration slightly increases from 93 to 95% with increasing NiO/CaO ratio while CH_4 concentration decreases. For NiO/CaO ratios above 0.7 the changes in H_2 and CH_4 concentration are negligible. As NiO/CaO ratio increases, more methane is oxidized from oxygen provided by the reduced NiO due to the increasing amount of NiO resulting in higher CH_4 conversions and H_2 purities. Furthermore, more CO_2 and less CO are produced with increasing oxidation of CH_4 by

NiO. As it can be observed from Figure 2.3b, the concentrations of CO_2 and CO are kept low, below 3% and they are equated when the ratio of NiO/CaO is equal to 0.5. As NiO increases in the reactor, the total oxidation of CH_4 is favored against the partial oxidation leading to lower CO concentrations at higher NiO/CaO ratios. On the other hand, CO_2 concentration is only affected by the equilibrium partial pressure over the solids. However as the amount of unreacted steam increases with higher NiO/CaO ratios, as less methane is consumed by the reforming reaction and H_2 production decreases (as shown below), the CO_2 concentration (in dry basis) will increase as a CO_2 partial pressure (in wet basis) lower than 0.158 cannot be achieved at 650°C.

An increase in the NiO/CaO ratio however also decreases H_2 yield during reforming as less CH_4 is consumed by the reforming reaction leading to a gradual reduction in the performance of SE – CL – SMR process. This decrease in hydrogen yield is plotted in Figure 2.4a as a function of the NiO/CaO ratio for SE-CL-SMR process together with methane conversion, while the reduction in the heat duty of the regenerator is presented in Figure 2.4b. Equilibrium H_2 yield, and CH_4 conversion of the simple SE-SMR process are also represented in the same figure for a NiO/CaO ratio equal to zero. As it can be observed, the addition of the NiO oxygen carrier is beneficial in sorption enhanced reforming. As NiO/CaO ratio increases, the thermal requirements of the regenerator are reduced and a higher H_2 purity is achieved due to the higher CH_4 conversions. Under specific conditions (higher NiO/CaO ratios) the regeneration cycle of the process can run under nearly auto-thermal conditions, with a penalty however in H_2 yield, as a higher part of CH_4 is consumed from the oxidation reactions.

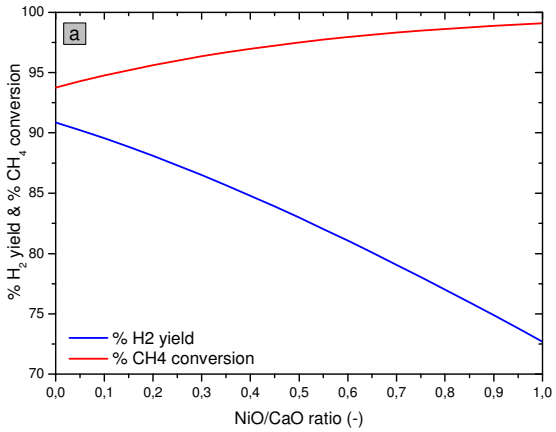

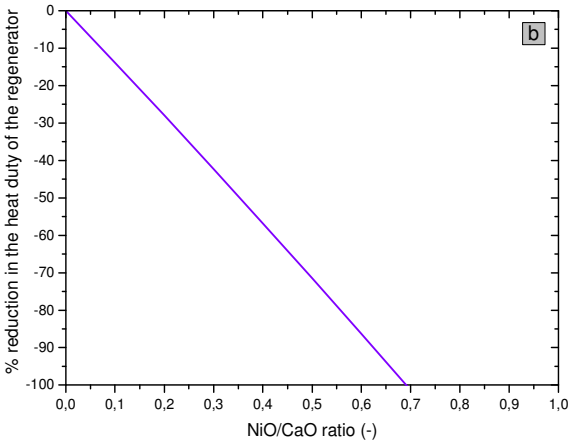

Figure 2.4: H_2 yield, CH_4 conversion and reduction in the heat duty of the reformer as a function of NiO/CaO ratio during SE-CL-SMR process (T = 650 °C, S/C ratio = 3, CaO/C = 1, NiO/CaO = 0-1).

3 Experimental Study

In this chapter, the experimental section of this thesis, conducted at the Laboratory of Petrochemical Technology of the Department of Chemical Engineering in the Aristotle University of Thessaloniki, is presented. The chapter contains a description of the experimental procedures followed (CO_2 sorbent and OTM synthesis, equipment and procedures used etc) and the presentation of the results of the experimental work. In the first part, results from the preliminary evaluation of the synthesized CaO-based CO_2 sorbent in a thermogravimetric analyzer (TGA) and the evaluation of the NiO-based catalytic activity in reforming reaction in a fixed bed flow unit are presented. The second part deals with the evaluation of the CO_2 sorbent combined with the NiO-based oxygen transfer material under sorption enhanced chemical looping reforming conditions in a fixed bed laboratory unit. The activity and stability of the materials was tested at different operating conditions (reforming temperatures, S/C ratios, OTM/sorbent ratios and residence times) and the results are presented in this order.

3.1 Experimental part

3.1.1 Synthesis

CaO–based CO_2 sorbent

The sorbent used in this study was a CaO-based CO_2 sorbent prepared from $Ca(NO_3)_2 \cdot 4H_2O$ (≥ 99.0 %, J.T. Baker) as a CaO precursor and $ZrO(NO_3)_2 \cdot xH_2O$ (99.5%, Acros) as a promoter's precursor using a sol-gel auto-combustion method and employing citric acid (≥ 99.0 %, J.T. Baker) as combustion agent according to the Reactions (3.1) and (3.2). The nitrate form of calcium and zirconium were chosen as precursors due to the fact that nitrates salts are known for their oxidizing properties and high solubility in water.

$$Ca(NO_3)_2 + \tfrac{5}{9}C_6H_8O_7 \rightarrow CaO + \tfrac{10}{3}CO_2 + \tfrac{20}{9}H_2O + N_2 \quad (3.1)$$

$$Ca(NO_3)_2 + ZrO(NO_3)_2 + \tfrac{10}{9}C_6H_8O_7 \rightarrow CaZrO_3 + \tfrac{20}{3}CO_2 + \tfrac{40}{9}H_2O + 2N_2 \quad (3.2)$$

Stoichiometric molar ratios of metal nitrates/combustion agent were chosen assuming that the by-products of the combustion reaction are only CO_2, H_2O and N_2, as shown in Reactions (3.1) and (3.2).

For the synthesis, firstly, an appropriate amount of metal nitrates was dissolved in distilled water under continuous heating and stirring. At a temperature of 70°C, a stoichiometric amount of the combustion agent was added to the aqueous solution of metal nitrates. Then the temperature was increased to ~120°C under continuous stirring leading to gelation. The formed gel was transferred to a pre-heated furnace at 300°C, where after a few minutes the gel auto-combusted in a self-propagating combustion manner resulting in the formation of a voluminous fluffy powder. The synthesized powder was then calcined at 900°C for 1.5 h with a heating rate of 10°C/min under air flow in order to remove the residual organic materials [36]. After calcination, the synthesized powder was sieved in order to obtain a particle size in the range between 180 and 355 μm. In Figure 3.1 different snapshots during the CO_2 sorbent synthesis are presented.

Figure 3.1: Snapshots during CO_2 sorbent's synthesis.

NiO/ZrO_2 oxygen carrier

The NiO-based oxygen transfer material (OTM) was prepared by wet impregnation of ZrO_2 support with an aqueous solution of nickel nitrate. The required amount of $Ni(NO_3)_2 \cdot 6H_2O$ (≥ 99.0 %, Merck) was dissolved in distilled water (50 mL) and mixed with the appropriate amount of support in a round bottom flask (Fig. 3.2) in order to achieve a loading of 40 wt% NiO. The mixture (green color) was heated for 1h slowly in a rotary evaporator under stirring at 70 °C. The solvent was then evaporated at 80-

85°C under reduced pressure. The obtained solid was dried overnight at 110 °C and then calcined at 650 °C for 4 h in air flow (10 °C/min) [45].

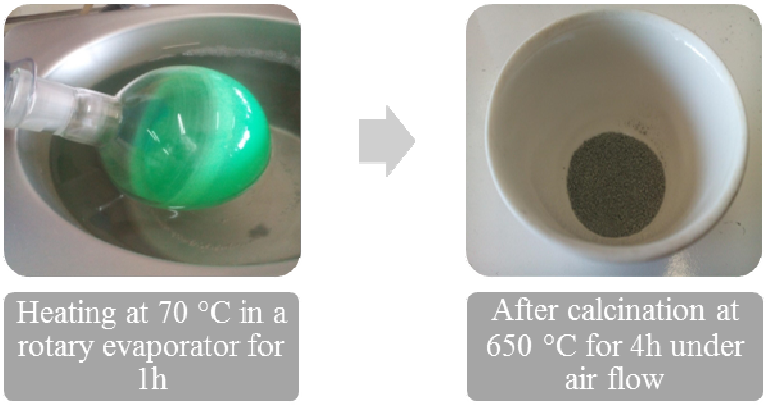

Figure 3.2: Snapshots during oxygen carrier's synthesis.

3.1.2 Preliminary evaluation of CO_2 sorbent in Thermogravimetric analyzer (TGA)

The sorption capacity and stability of the CaO-based CO_2 sorbent was examined under a TGA, in a SDT Q600 instrument for 100 continuous sorption-desorption cycles. The sorption capacity of the synthesized sorbents was examined under 15% CO_2 flow in N_2 for 30 minutes at 650°C while desorption occurred with 100% N_2 flow for 5 minutes at 850°C. The selection of CO_2 concentration was based on the realistic concentration of CO_2 in the outlet stream of the reformer, which does not exceed 15% at 650°C. Results are presented regarding the weight increase of the materials and CaO conversion. CaO conversion can be expressed according to weight increase of the sorbent due to CO_2 absorption:

$$X(t), \% = \frac{weight\ increase\ (t)}{0.785} \cdot \frac{1}{w_{CaO}} \tag{3.3}$$

where 0.785 is the maximum theoretical weight increase for complete conversion of CaO to $CaCO_3$ and w_{CaO} is the weight fraction of free CaO (0.66) present in the sorbent [46].

3.1.3 Preliminary evaluation of OTM's catalytic activity under conventional reforming conditions

The evaluation of the NiO-based OTM's catalytic activity in reforming reaction was performed at atmospheric pressure in the bench scale laboratory flow unit described below. About 50 mg of material diluted with a predetermined amount of quartz particles was loaded in the reactor, in order to achieve a Gas Hourly Space Velocity of 100,000 h^{-1}. The sample was initially heated to 650°C under He flow, followed by in-situ reduction in 33% H_2/He for 1 hour at 650°C in order to obtain the metallic form of nickel. After the reduction, reforming was performed by switching to CH_4 and steam flow, with S/C molar ratio of 3. The reaction was conducted isothermally at 650 °C for 10 hours.

The performance of the OTM is expressed in terms of CH_4 conversion (X_{CH_4}) which was calculated with the following equation:

$$X_{CH_4}(\%) = \frac{CO_{out} + CO_{2,out}}{CH_{4,out} + CO_{out} + CO_{2,out}} \times 100 \quad (3.4)$$

3.1.4 Description of fixed bed laboratory unit for activity testing

A schematic representation of the fixed bed laboratory unit is presented in Figure 3.3. The unit consists of the liquid and gas feed inlet section, the reactor and the product analysis section. The incoming gases are controlled via mass flow controllers and are mixed before entering the reactor. Distilled water (steam) is admitted to the reactor through a pre-heater using an HPLC pump. For the experiments, a fixed bed quartz reactor (12mm external diameter) is used equipped with a coaxial thermocouple for temperature monitoring. The reactor is heated electrically by a three zone tubular furnace. Each temperature zone can be independently controlled. The exit gases from the reactor are cooled down to condensate the unreacted steam.

The gas phase products are analyzed by an online gas chromatograph (Agilent Technologies, 7890A) which has a thermal conductivity detector. More specifically, the output gas stream is analyzed using two columns (Molecular Sieve and Poraplot) in series by pass configuration. The Molecular Sieve column is used for the separation of H_2, CH_4 and CO and the Poraplot for the detection of CO_2. The CO and CO_2 concentrations exit of the reactor are also monitored by a gas analyzer (Madur, Mamos-200) [47].

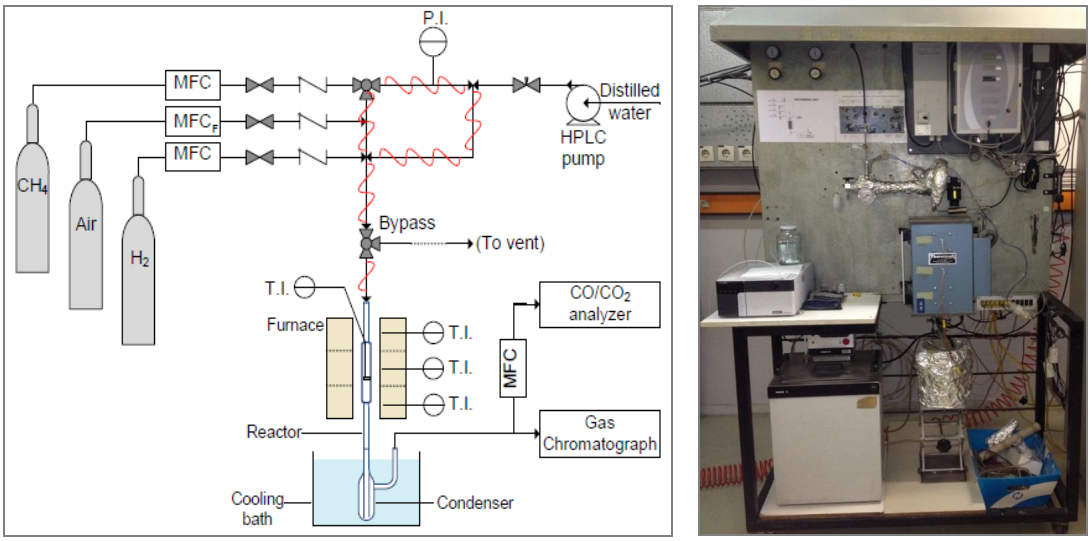

Figure 3.3: Schematic layout of the fixed bed bench scale unit.

3.1.5 Reaction performance evaluation – Operating conditions

A mechanical mixture of NiO/ZrO_2 and $CaO/CaZrO_3$ was loaded in the reactor. The materials were initially heated to 800 °C under air flow (160 cm^3/min) in order to refresh the sorbent and ensure that the OTM is in its oxidized state. The reactor was cooled down to the reforming temperature and the materials were exposed to CH_4/steam. During the first 15 min of the reduction/reforming step a small external H_2 flow was added in the feed stream in order to facilitate NiO reduction. The evolution of the products (H_2, CO and CO_2) was monitored online by a gas chromatograph. The CO and CO_2 concentrations in the reactor exit were also monitored by a gas analyzer. The reaction was run isothermally at the reforming temperature until the sorbent was saturated. After saturation of the sorbent, the feed was switched to air (160 cm^3/min) and the temperature of the reactor was raised to 800 °C for reoxidation of NiO and regeneration of the saturated sorbent. Between the two stages He flow was introduced in the reactor at constant temperature (reforming temperature) until CO and CO_2 concentrations in the analyzer reached ~zero.

3.1.6 Post reaction characterization of the materials

In order to understand the changes occurring on the sorbent and the OTM during the multiple cycles of SE-CL-SMR experiment, the characterization of both fresh and spent materials was performed. This section presents briefly the methods of characterization that were used during this thesis.

Specific surface area and pore volume were measured by using nitrogen physisorption at 77 K with an Autosorb-1 Quantachrome flow apparatus. Prior to the measurements, the samples were degassed in vacuum at 250 °C overnight. The Brunauer-Emmett-Teller (BET) method is a widely used and established approach of determining the specific surface area of solid materials, especially such with distinct open porosity. It is based on physical adsorption of an inert gas, usually nitrogen on its surface at the liquid nitrogen temperature of 77.4 K. Each adsorbed molecule covers on the surface of porous material, an area equal to its cross section. In the case of nitrogen, the sectional area of the molecule is equal to 16.2 $Å^2$. If the amount of adsorbates required for a hypothetic densely packed monomolecular layer at the surface of the sample and the area covered by a single adsorbate molecule are known, the magnitude of the surface may be established.

X-ray diffraction (XRD) patterns were obtained with a Siemens D500 diffractometer and Cu Kα radiation with radiation wavelength of 0.15406 nm. An aluminum holder was used to support the samples during the measurements. The intensity data were collected over a 2h range of 5–80° with a step of 0.04° and a scanning rate of 2 s/point. X-ray diffraction (XRD) is a common technique used for phase identification of crystalline solid materials. It is based on interaction of monochromatic X-rays and a crystalline sample. These X-rays are directed at the sample, and then the diffracted rays are collected. A key element is the angle between the incident and diffracted rays [48].

3.2 Results and discussion

3.2.1 Preliminary evaluation of the materials

CaO-based CO_2 sorbent

The sorption capacity and stability of the CaO-based CO_2 sorbents was evaluated in multiple carbonation/calcination cycles in a TGA apparatus. Sorption was performed at 650°C for 30 min in 15%CO_2/N_2 flow, while desorption took place at 850°C for 5 min in N_2. The carbonation conversion of the promoted CaO sorbent as a function of number of cycles is presented in Figure 3.4. The synthetic Zr-promoted sorbent exhibits very stable performance during the 100 cycles with less than 14% deactivation in contrast to CaO derived from natural limestone [32-37] which shows a rapid loss of conversion even after only a few cycles. In addition to stability, the chosen synthesis method leads to the formation of a CaO-based sorbent with an enhanced initial sorption capacity of 10.6 moles of CO_2/kg of sorbent which corresponds to ~90% conversion of the free CaO in the sorbent.

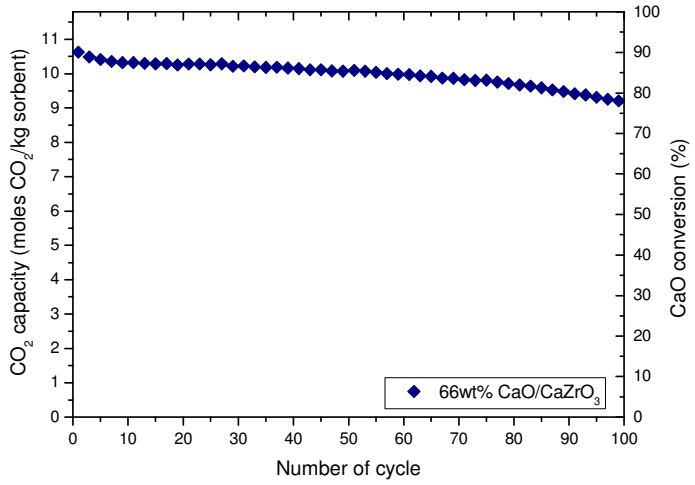

Figure 3.4: CO_2 capacity and CaO conversion of the synthetic CaO sorbent as a function of number of cycles (Carbonation: 650 °C, 15% CO_2/N_2, 30 min, Calcination: 850 °C, 100% N_2, 5 min).

NiO-based Oxygen Carrier

A suitable oxygen carrier for sorption enhanced chemical looping steam methane reforming should exhibit good reforming activity in its reduced form. Therefore, NiO/ZrO_2 was pre-reduced in situ and was then tested as a conventional reforming catalyst in steam methane reforming at 650°C with S/C ratio of 3. In Figure 3.5, methane

conversion over reduced NiO/ZrO_2 is plotted as a function of time-on-stream. The catalyst has a satisfactory activity, with a high initial methane conversion of ~80%, which is quite close to thermodynamic equilibrium (dashed line) taking in to account the very low residence time of the feed stream in the catalytic bed (GHSV=100,000h^{-1}) and a good stability with approximately 8% relative decrease in conversion after 10 hours on stream.

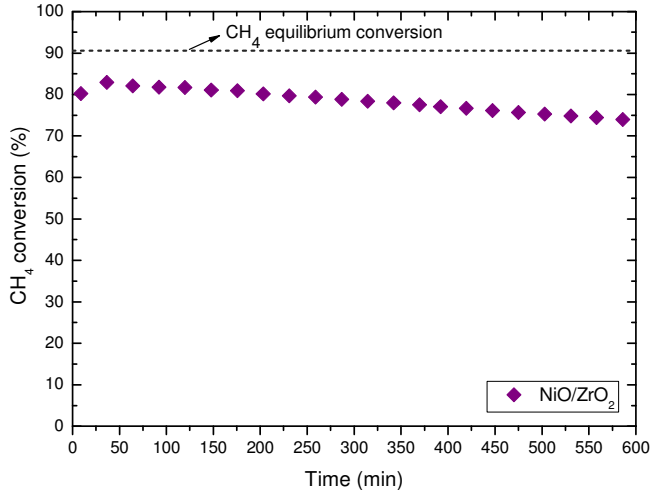

Figure 3.5: Methane conversion as a function of time for zirconia supported OTM (Reduction/Reforming: T = 650 °C, S/C ratio = 3, GHSV = 100,000 h^{-1}, Oxidation: T = 850 °C).

3.2.2 Sorption enhanced-chemical looping reforming experiments: Parametric study

The two materials, $CaO/CaZrO_3$ and NiO/ZrO_2 exhibited high sorption capacity and catalytic activity respectively, very good stability in multiple cycles and were further tested under sorption enhanced chemical looping reforming conditions. In order to determine the effect of crucial parameters, such as reforming temperature, H_2O/CH_4 (S/C) ratio, NiO/CaO (OTM/Sorbent) ratio and residence time of the feed stream in the reactor, a parametric study was contacted on a range of these parameters testing the activity and stability of the materials at different operating conditions. The type and range of these parameters for the reforming/reduction/carbonation cycle are tabulated in Table 3.1.

Table 3.1: Range of investigated parameters.

Temperature [°C]	**H_2O/CH_4 (S/C) ratio**	**NiO/CaO ratio (OTM/sotbent)**	**Residence time GHSV [h^{-1}]**
600, 650, 700	2, 3, 4	0.2, 0.5, 0.8	255, 531, 797, 1063

Effect of temperature

During sorption enhanced chemical looping steam methane reforming experiments, a mechanical mixture of OTM/catalyst in its oxidized state and CaO-based sorbent with a NiO/CaO molar ratio of 0.5 was exposed to steam and methane flow with S/C ratio equal to 3 until complete saturation of the CO_2 sorbent (approximately 90-120 min depending on the reforming temperature). For the first 10 minutes was also fed externally supplied hydrogen (5% of the total feed), in order to facilitate the reduction of NiO to metallic Ni. Following the step of reforming, the reduced oxygen carrier (metallic nickel) is re-oxidized under air flow and the sorbent is regenerated at the same temperature (800 °C) in a single reactor.

In SE – CL – SMR (sorption enhanced chemical looping steam methane reforming) occur simultaneous endothermic and exothermic reactions, rendering temperature an important contributor to the equilibrium of the reforming reactor. A range of temperatures was examined to find the optimal operating temperature for the reforming reactor. The main findings of the experimental study were compared to those revealed from the simulation study. In the following Figure 3.6 the effect of temperature in the experimental and equilibrium product concentrations (% H_2, CH_4, CO_2 and CO) is depicted during the reduction/reforming stage over NiO/ZrO_2 and $CaO/CaZrO_3$.

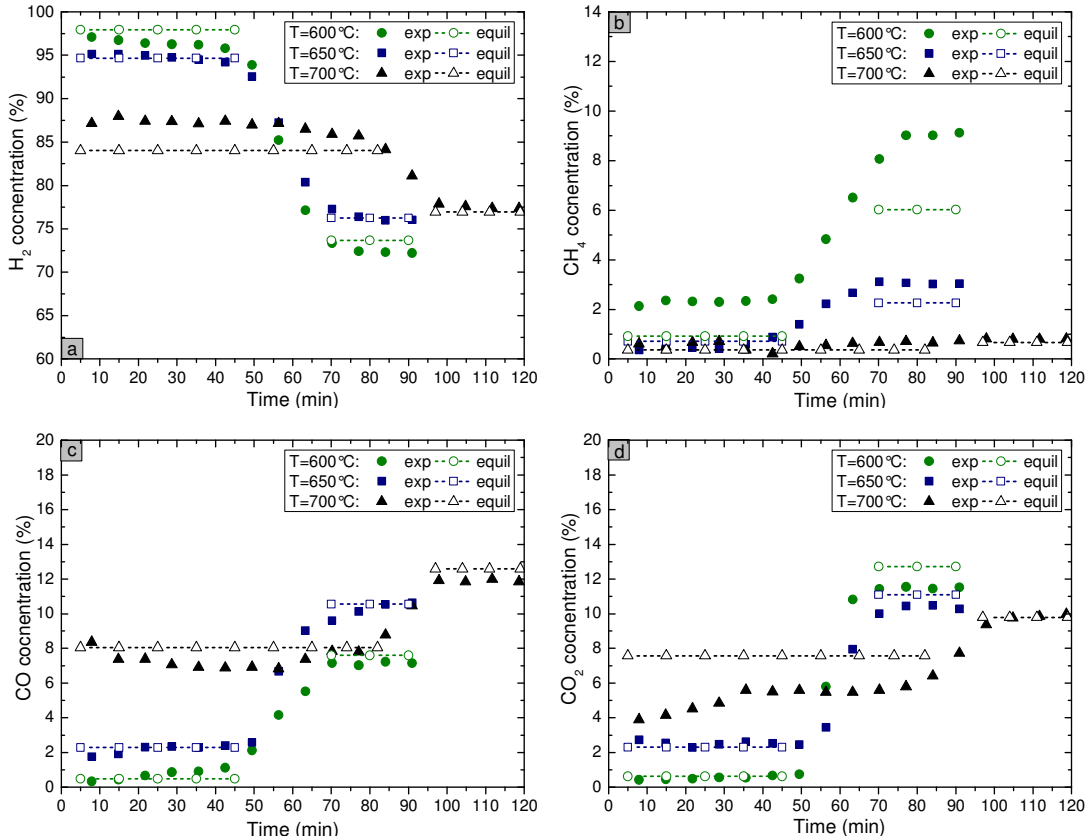

Figure 3.6: Experimental and equilibrium product concentrations [(a) H_2, (b) CH_4, (c) CO and (d) CO_2] in the outlet of the reactor as a function of time during the reduction/reforming stage over NiO/ZrO_2 and $CaO/CaZrO_3$ (T=600°C, 650°C, 700°C, S/C ratio=3, NiO/CaO=0.5, GHSV=255 h^{-1}).

As it can be observed in Figure 3.6, experimental product concentrations closely follow the same general trend as the equilibrium product concentrations at three different temperatures. Three regions, i.e. prebreakthrough, breakthrough, and postbreakthrough, are observed. During the prebreakthrough period, NiO reduction, reforming and water gas shift reaction are carried out simultaneously with in situ CO_2 removal by the sorbent. At this period, H_2 concentration is very high, while the CO and CO_2 concentrations are low. After that period, at the breakthrough region, sorbent is gradually saturated and CO_2 removal is less effective. In addition, the CO, CO_2 and CH_4 concentrations increase, while the H_2 concentration decreases. When the sorbent is nearly completely saturated, the postbreakthrough period starts, where the capture of the produced CO_2 is considered negligible and the product concentration of the reformer turns into that of conventional reforming.

More specifically, in the prebreakthrough period, the product concentration at higher temperature contains less CH_4 and H_2, but more CO and CO_2. A high H_2 purity, over 88% is obtained for all temperatures, with values exceeding 95% for temperature lower than 650°C. This is expected as higher temperatures favor higher conversion of CH_4 during both prebreakthrough and postbreakthrough period, because of the strongly endothermicity of the reforming reaction, while the efficiency of the CO_2 sorbent declines as the exothermic carbonation reaction is limited by the temperature, leading to lower shift of the reforming and the WGS reactions and a decrease of H_2 concentration. Similarly, at higher temperatures the exothermic water gas shift reaction is not favored, leading to higher concentration of CO in both prebreakthrough and post breakthrough period. After saturation of the sorbent (postbreakthrough period), higher temperature results in higher concentrations of H_2 and CO, but lower concentrations of CH_4 and CO_2, as the product composition is only limited by the equilibrium of reforming and water gas shift reactions [49].

Even though the high temperature is not favorable for the capture of CO_2, a lower CO_2 concentration compared to equilibrium is achieved during the prebreakthrough period at 700°C. This can be attributed to the fact that during the experiment, a wide temperature profile was established throughout the entire material bed (670-700°C). The lower temperature at different positions of the bed resulted in enhancing the carbonation conversion and leading to lower CO_2 concentration and higher H_2 purity compared to thermodynamics at this temperature.

The positive effect of the addition of CO_2 sorbent is clearly demonstrated when comparing the CH_4 concentrations in the outlet of the reactor at the different temperatures. Higher temperatures favors higher methane conversions during both prebreakthrough and post breakthrough period, due to the strongly endothermicity of the reforming reaction, with CH_4 concentrations at 650 and 700°C reaching the equilibrium. At 600°C, even in the presence of the sorbent CH_4 concentration is higher compared to equilibrium (~2.3% instead of 0.92%) with an equivalent decrease observed in H_2 concentration, indicating that the reforming reaction is strongly restricted by the low temperature. This deviation however is more pronounced after the progressive saturation of the sorbent (post breakthrough period).

After the reforming/reduction step, the reduced oxygen carrier is re-oxidized under air flow and the sorbent is regenerated at the same temperature (800 °C) in a single reactor. In Figures 3.7 and 3.8 the temperature profiles and CO_2 concentrations for three different temperatures during the reoxidation/calcination stage are shown.

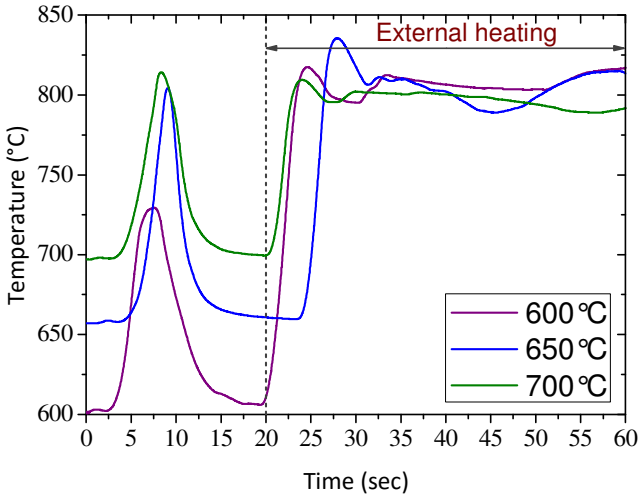

Figure 3.7: Temperature profile during the reoxidation/calcination stage.

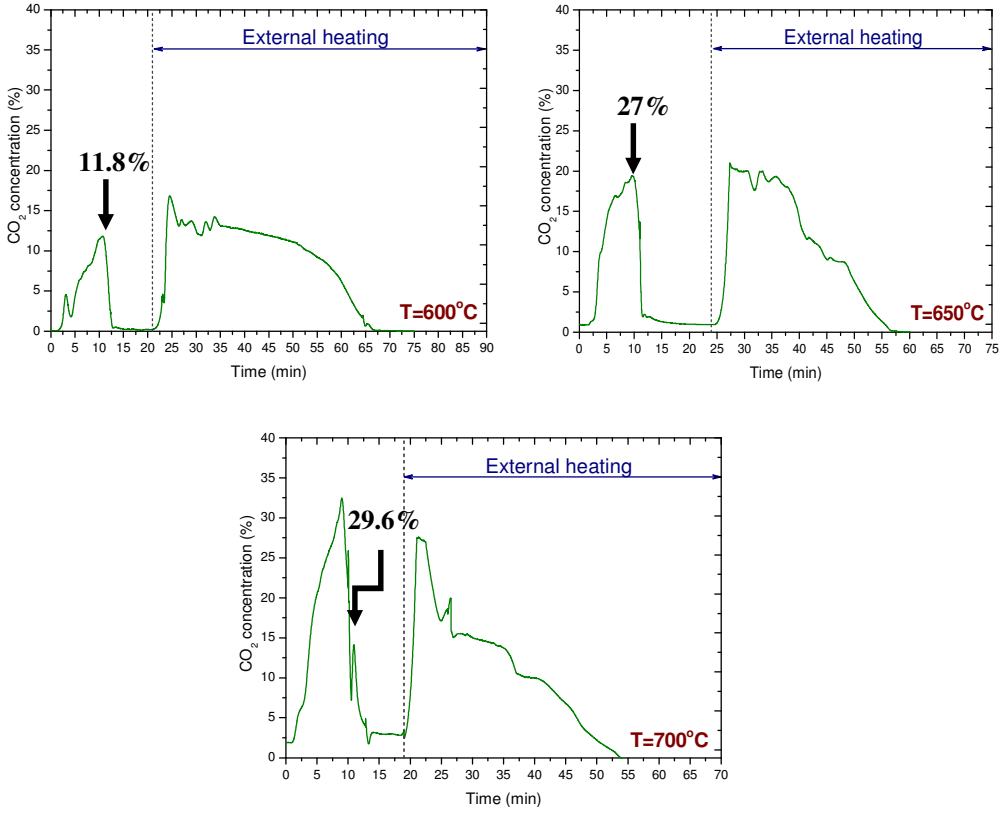

Figure 3.8: CO and CO_2 concentrations as a function of time at three different reforming temperatures during the reoxidation/calcination stage (T_{ref}=600°C, 650°C, 700°C, S/C ratio=3, NiO/CaO=0.5, GHSV=255h^{-1}, T_{reg}=800°C).

As it can be observed from Figure 3.7, during the initiation of the reoxidation/regeneration step the temperature increases at three different reforming temperatures without having applied additional external heating to the reactor. This happens due to the heat generated by the highly exothermic reaction of the reoxidation of the reduced Ni. Due to this heat generation, the temperature of the reactor increases by ~150°C, and a part of the saturated sorbent is regenerated simultaneously due to the increased temperature. When a low temperature was used during reforming (600°C) the maximum temperature reached during Ni reoxidation was lower than 750°C. At these temperatures $CaCO_3$ calcination occurs with lower rates, resulting in a limited release of CO_2 during the same period that Ni oxidation occurs (~12% of the total CO_2 released). On the other hand when regeneration starts at higher temperatures (650 and 700°C) the maximum temperature reached was much higher (>800°C) and hence more than twice of CO_2 (27 and 29.6% as compared to 11.8%, respectively) is released simultaneously with Ni oxidation.

Even though the highest temperature due to Ni oxidation was recorded during the third case ($T_{reforming}$=700°C) as expected, compared to the second case ($T_{reforming}$=650°C), the temperature increase was lower ($\Delta T \approx 119$°C instead of 143°C) leading to a proportionally low increase of the percentage of CO_2 that is desorbed at the same time (from 27 to ~30%). This difference could be attributed to the rate of the $CaCO_3$ calcination occurring simultaneously. As the rate of $CaCO_3$ that is decomposed is higher when regeneration stage initiates at higher temperature (T=700°C), the abduction of the heat generated by the exothermic Ni oxidation from the highly endothermic decomposition reaction is higher, inhibiting this way the further increase of the reactor's temperature.

Effect of S/C ratio

Steam is a reactant in both reforming and water gas shift reaction, as a result a change in (S/C) ratio can affect the equilibrium of these two reactions. A range of (S/C) ratios was tested to find the optimal for the reforming reactor. In the following Figure 3.9 the effect of (S/C) ratio on the experimental and equilibrium concentration (% H_2, CH_4, CO_2 and CO) during the reduction/reforming stage is depicted for three different ratios of 2, 3 and 4. The experiment with steam to carbon ratio equal to two was carried out by doubling the flows in order to achieve a constant water flow in the pump.

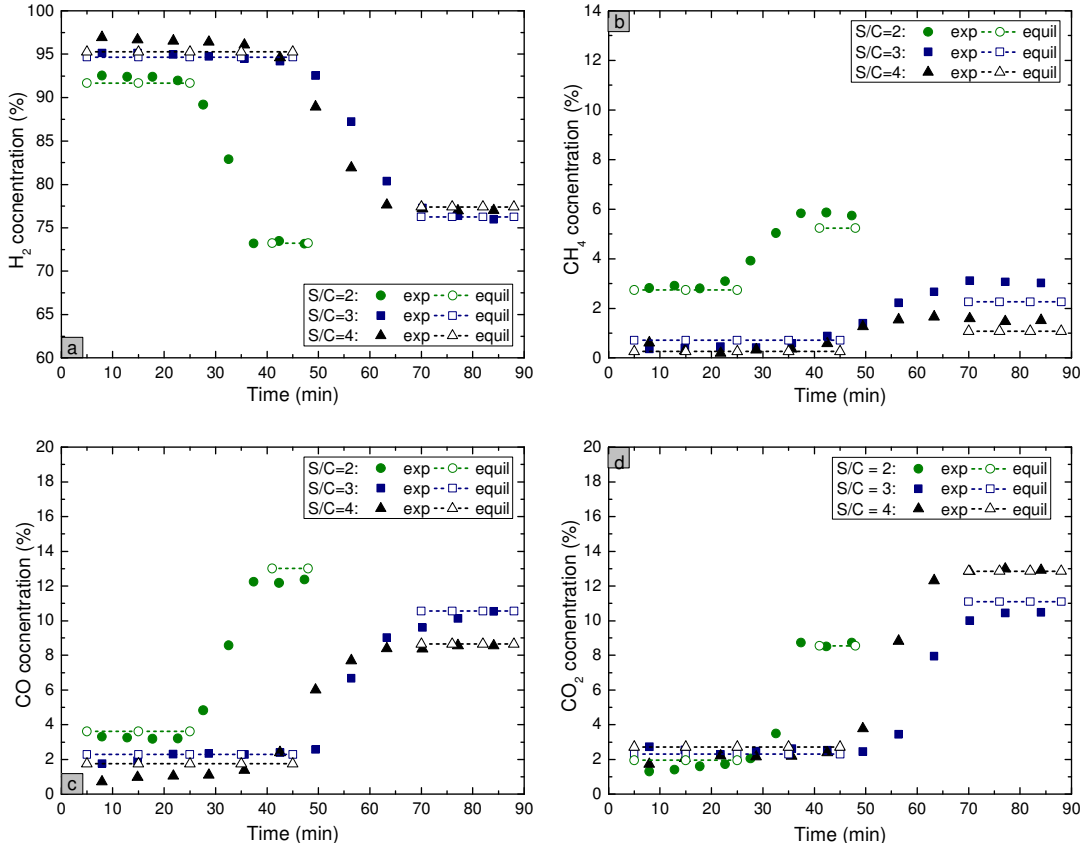

Figure 3.9: Effect of steam to carbon ratio in the reactor's product concentrations [(a) H_2, (b) CH_4, (c) CO and (d) CO_2] during the reduction/reforming stage over NiO/ZrO_2 and $CaO/CaZrO_3$ (S/C ratio = 2, 3, 4, T = 650°C, NiO/CaO = 0.5, GHSV = 400 h^{-1}, 255 h^{-1}, 319 h^{-1}).

Based on the above figure (Fig. 3.9), the experimental data are in good agreement with the simulated results. An increase of S/C ratio shifts both WGS and reforming reactions to the product side, resulting in the production of H_2 with higher purity. More specifically, during the prebreakthrough period, the concentration of H_2 increases with higher (S/C) ratio from ~92% to ~97% for an increase in S/C ratio from 2 to 4. In all cases slightly higher H_2 concentrations were achieved during the experiments compared to equilibrium. The differences however are very low within the experimental error.

The shift of WGS reaction to the right at higher S/C ratios increases CO consumption and CO_2 production [50]. This leads to a slight increase of CO_2 concentration with higher S/C ratio. However this increase is very low in the range of S/C ratios studied (<1%) and it is not clearly observed in the experimental data during the prebreakthrough period, while the difference in CO_2 concentrations is more pronounced after complete saturation of the sorbent (post breakthrough) where compositions of conventional reforming process are achieved. Even though CO_2 concentration increases with S/C ratio,

when the overall carbon balance in the system is taken into account, the excess of steam leads to higher CO_2 capture efficiency. The higher CO_2 capture would lead to faster saturation of the sorbent material which is observed in the slight decrease of the duration of the prebreakthrough period with higher S/C ratios (when comparing experiments performed using the same CH_4 flows (S/C 3 and 4).

By increasing (S/C) ratio (excess of steam), reforming and water gas shift reactions are shifted to the same direction to the products side. Higher (S/C) ratio is favorable for higher outlet concentration of H_2, thus improving process efficiency. At the same time, steam addition facilitates WGS reaction [28]. The shift of WGS reaction to the right increases CO_2 production and CO consumption. The excess of steam not only favors the thermodynamics of the reforming reaction but also inhibits coke deposition. However, a large excess of steam induces an efficiency penalty due to higher energy demands for steam generation [51]. Therefore, based on the above, an intermediate S/C ratio close to 3 is preferred.

Effect of OTM/sorbent ratio

The utilization of NiO in the reforming reactor and the re-oxidation step of metallic Ni in the regenerator are those that separate the SE-SMR from SE-CL-SMR, as the exothermic oxidation reaction of Ni to NiO produces a large percentage of the total energy required for the calcination of the saturated sorbent. A range of molar NiO/CaO ratios was examined to find the optimal one for the reforming reactor. In the following figure 3.10 the effect of NiO/CaO in the experimental and equilibrium product concentration (% H_2, CH_4, CO_2 and CO) is presented over time during the reduction/reforming stage for three different NiO/CaO ratios of 0.2, 0.5 and 0.8.

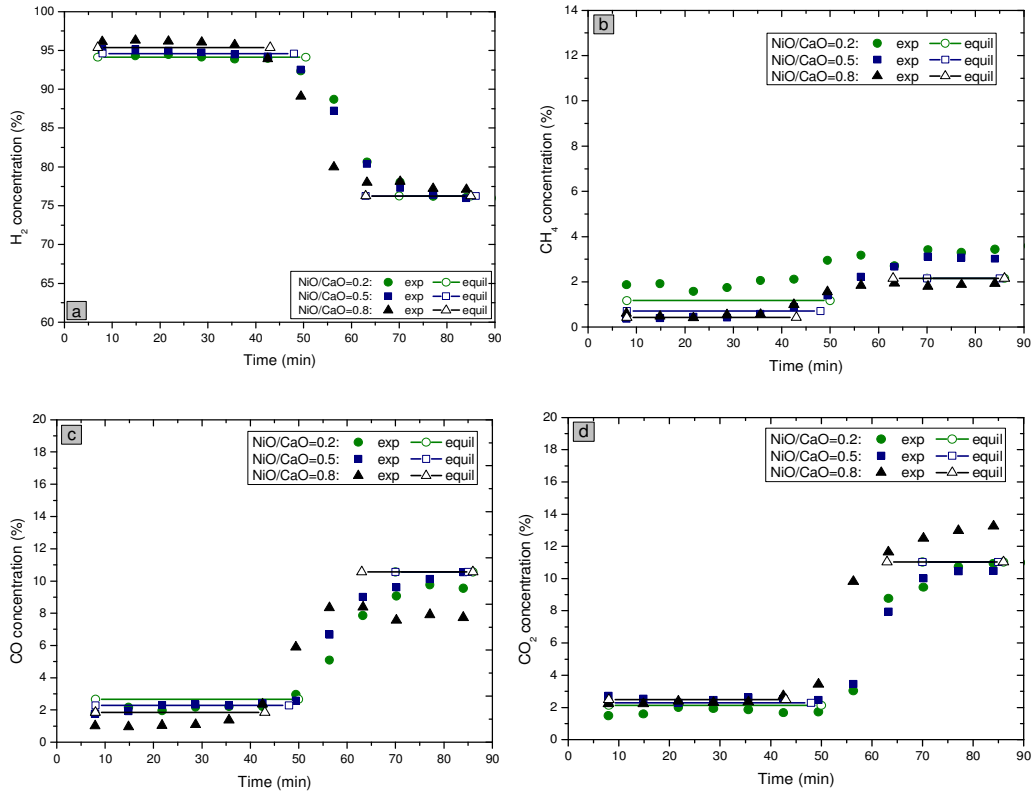

Figure 3.10: Effect of NiO/CaO ratio in the reactor's product concentrations [(a) H_2, (b) CH_4, (c) CO and (d) CO_2] during the reduction/reforming stage (NiO/CaO ratio = 0.2, 0.5, 0.8, T=650°C, S/C = 3, GHSV = 288 h^{-1}, 255 h^{-1}, 230 h^{-1}).

Based on the above figures, experimental and equilibrium results follow the same trend. At the prebreakthrough period, H_2 concentration slightly increases with increasing NiO/CaO ratio while CH_4 concentration decreases. According to the thermodynamics of the participating reactions, as NiO/CaO ratio increases, more methane is oxidized due to the increasing amount of NiO and less is consumed by the reforming reaction. As more CO_2 is produced with increasing oxidation of CH_4 by the oxygen carrier, its partial pressure increases and the equilibrium of the carbonation reaction is shifted to the products side. As a result, a high purity H_2 stream is produced [43]. More specifically, as the NiO/CaO ratio increases from 0.2 to 0.8, a higher H_2 purity is achieved (95.7% instead of 94 %) with a corresponding reduction in CO and CH_4 concentrations. At the postbreakthrough period, H_2 concentration remains the same for the three different NiO/CaO ratios, something expected due to the reduction of NiO to Ni. Furthermore, CH_4, CO_2 and CO concentrations are respectively close for the NiO/CaO ratios of 0.2 and 0.5. However, at the NiO/CaO of 0.8, the concentrations of CH_4, CO_2 and CO diverge. This deviation however is very low (<2%) and could be attributed to experimental errors. After sorbent's gradual saturation (breakthrough region), it was difficult to maintain a

constant temperature during the first minutes of the post breakthrough period due to the endothermicity of the reforming reaction, leading to these discrepancies in the products concentrations.

The beneficial effect of NiO/CaO ratio in the SE-CL-SMR process is clearly shown in the thermal requirements of the regeneration stage. After the reforming/reduction step, the reduced oxygen carrier is re-oxidized under air flow and the sorbent is regenerated at the same temperature (800 °C) in a single reactor. The CO_2 concentrations at three different OTM/sorbent ratios during the reoxidation/calcination stage are presented in Figure 3.11.

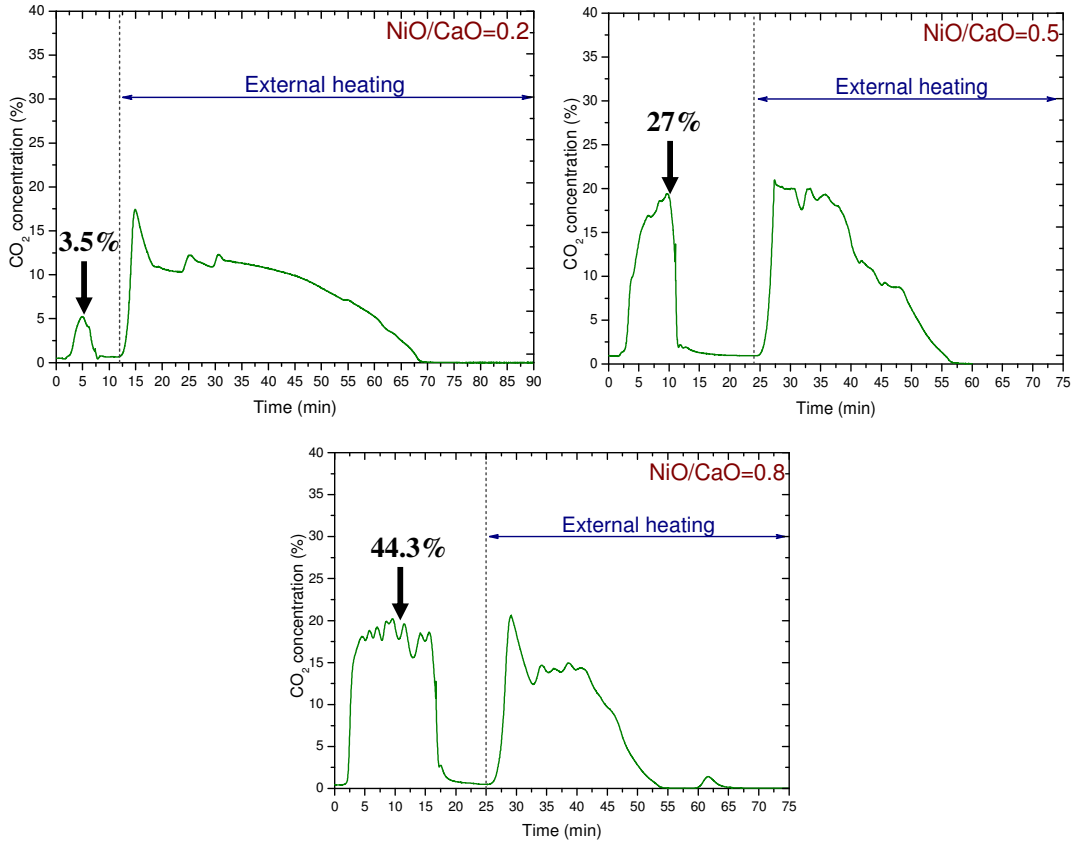

Figure 3.11: CO and CO_2 concentrations as a function of time at three different NiO/CaO ratios during the reoxidation/calcination stage (NiO/CaO = 0.2, 0.5, 0.8, T_{ref} = 650°C, S/C = 3, GHSV = 288, 255, 230h^{-1}, T_{reg} = 800°C.

The oxidation of the reduced Ni is a highly exothermic reaction so the heat generated from the reoxidation of Ni can cover a part of the heat required for the regeneration of the sorbent. When a low NiO/CaO molar ratio of 0.2 was used the heat generated by

Ni reoxidation was not sufficiently high and the maximum temperature recorded in the reactor was lower than 740°C. At these temperatures calcination of $CaCO_3$ occurs at lower rates, leading to desorption of only ~3% of the captured CO_2 at the same period that Ni reoxidation takes place. When NiO/CaO ratio was increased to 0.5 and 0.8 the temperature of the reactor reached a maximum value of 803 and ~820°C respectively, with a respective increase of the duration of Ni oxidation period from ~10min to 17 and 23min. At the same time the percentage of the heat required for sorbent's regeneration that is covered in-situ by the exothermic oxidation reaction increases to 27 and ~45% for NiO/CaO ratios of 0.5 and 0.8 respectively.

Effect of residence time

A range of residence times was examined to find the optimal one for the reforming reactor. In the following Figure 3.12 the effect of feed space velocity (gas hourly space velocity GHSV) on the product concentration (% H_2, CH_4, CO_2 and CO) during the reduction/reforming stage is shown. The feed space velocity was varied by changing the inlet flow rate of CH_4 from 24 to 100 ml/min but maintaining the ratio of H_2O/CH_4 equal to 3.

It can be seen from Fig. 3.12 that an increase of the GHSV results in a decrease of the prebreakthrough period as it was expected. Very high H_2 concentrations were recorded regardless the increase of spatial velocity in the experiments, demonstrating the high capability of the $CaO/CaZrO_3$ sorbent to remove the produced CO_2, even when lower conduction times were applied, shifting the global reaction to values near equilibrium. When GHSVs higher than $797h^{-1}$ were used, a slight increase in CH_4, CO and CO_2 concentrations was observed, which were however still very close to equilibrium. The variation of GHSV does not seem to affect the catalytic activity of the oxygen carrier. Even during the post breakthrough region where the effect of the sorbent was negligible, a gas composition very close to equilibrium was achieved.

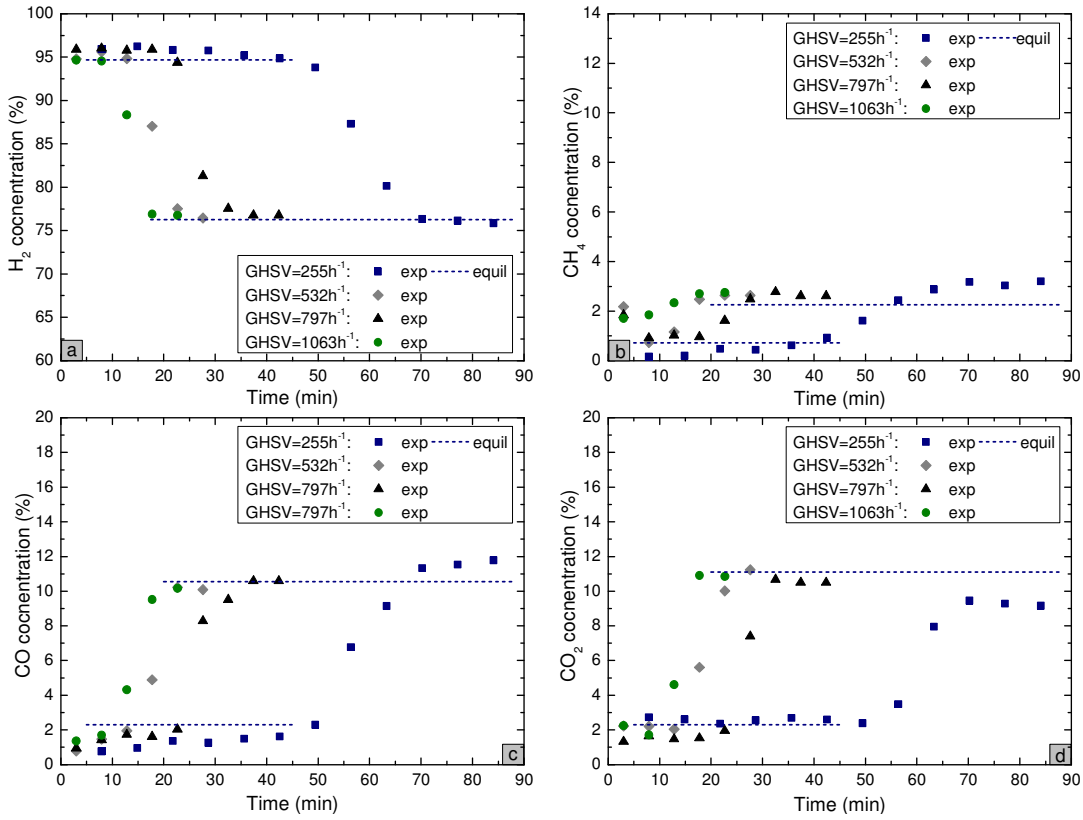

Figure 3.12: Effect of residence time in the reactor's products concentrations [(**a**) H_2, (**b**) CH_4, (**c**) CO and (**d**) CO_2] over NiO/ZrO_2 OTM and $CaO/CaZrO_3$ CO_2 sorbent (T=650°C, S/C ratio=3, NiO/CaO molar ratio=0.5, GHSV=255 h^{-1}, 532 h^{-1}, 797 h^{-1}, and 1063 h^{-1}).

3.2.3 Stability test under SE-CL-SMR conditions

The stability of the materials under cyclic SE-CL-SMR operation was tested for 20 reduction/reforming and regeneration cycles. The reforming stages were carried out at 650°C and atmospheric pressure in CH_4/steam while regeneration of the materials was performed by increasing the temperature to 800°C under air flow. Figure 3.13a shows the average H_2 concentration during the prebreakthrough period as well as the duration of this region during the 20 SE-CL-SMR cycles.

A high H_2 concentration over 92 % was achieved during almost all the cycles, indicating that there was not significant deterioration in the performance of the OTM/catalyst and the CO_2 sorbent material. This is also evident by the almost constant time of the prebreakthrough region with increasing number of cycles. This is clearer when CaO conversion is plotted versus the number of cycle (Figure 3.13b). Data from the preliminary test of the sorbent in TGA are represented for comparison reasons. CaO conversion was calculated based on the amount of CO_2 that was desorbed during regeneration stage. The material exhibits a high carbonation conversion of the free CaO (~87.8%)

during the first cycle with very a low loss of capacity after 20 cycles, with only ~4.6% deactivation. Comparing these values with the results obtained from the preliminary testing of the material in a TGA apparatus, it can be seen that the sorbent retains almost completely its intristic initial capacity and demonstrate a similar stability even when it is exposed for prolonged periods under calcination conditions in the bench scale experiments (~60min compared 10 min in the TGA tests). This is very crucial, as the activity and stability of the sorbent material are considered as key challenges for successful commercialization of high temperature CO_2 removal applications. Especially in the case of catalytic processes such as SE-CL-SMR, the stability of the sorbent material is considered as the most important parameter, as it should be compatible with the stability of the OTM/catalyst under multiple cycles.

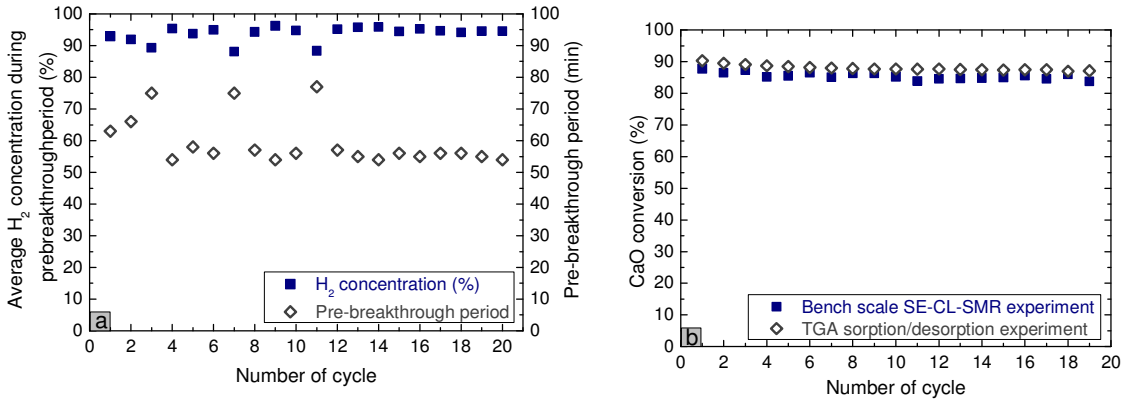

Figure 3.13: H_2 purity and duration of prebreakthrough period (a) and CaO conversion of 66%CaO/CaZrO3 (b) during 20 consecutive SE-CL-SMR cycles (reforming stage: T=650°C, S/C ratio=3, NiO/CaO molar ratio=0.5, GHSV=255 h^{-1} regeneration stage: T=650°C→800°C, air flow).

3.2.4 Post-reaction characterization

The 20th cycle was terminated after the reduction/reforming/carbonation stage and the two materials were separated using a magnet to extract the reduced oxygen carrier. A detailed characterization of physicochemical properties of the used materials was performed separately in order to support the previous results.

The surface area and pore volume of the fresh and used $CaO/CaZrO_3$ and NiO/ZrO_2 are presented in Table 3.2. The surface area and pore volume of the fresh $CaO/CaZrO_3$ after the initial calcination at 900°C were found to be 21 m^2/g and 0.20 cm^3/g, respectively. After the reduction/reforming/carbonation stage of the 20th cycle, the surface

area of carbonated $CaO/CaZrO_3$ decreases to ~4 m^2/g due to the pore blockage by the captured CO_2. However after calcination, the surface area and pore volume of the spent material restore to 19.2 m^2/g and 0.19 cm^3/g, values similar to the one calculated for the fresh sorbent. The very low decrease in surface area of the material after cycling is in very good agreement with the significantly stable performance of the sorbent during the 20 SE-CL-SMR cycles that corresponds to more than 60 h under experimental conditions. On the other hand the surface area of the oxygen carrier was drastically reduced from 26.3 m^2/g to 9.3 m^2/g. This can be expected, considering that due to the very high loading of NiO (40 wt %) the material is more prone to sintering at the high temperatures during the experiment. The reduced surface area however does not affect the catalytic activity of the material as due to the high amount of oxygen carrier used in the experiments, equilibrium conditions were achieved in the reactor.

Table 3.2: BET surface area and pore volume of fresh and used $CaO/CaZrO_3$ and NiO/ZrO_2

	Surface area (m^2/g)	**Pore volume (cm^3/g)**
$CaO/CaZrO_3$ fresh-calcined	21.0	0.20
$CaO/CaZrO_3$ used-carbonated	3.9	0.02
$CaO/CaZrO_3$ used-calcined	19.2	0.19
NiO/ZrO_2 fresh-oxidized	26.3	0.16
NiO/ZrO_2 fresh-reduced	9.3	0.13

The X-ray diffraction patterns of the fresh and used materials, $CaO/CaZrO_3$ and NiO/ZrO_2, are illustrated in Figures 3.14 (a) and (b) respectively. Characteristic reflections of CaO appear in the XRD spectra of the fresh calcined sorbent, along with low intensity peaks of $Ca(OH)_2$ that are attributed to the absorption of moisture due to the hydroscopic nature of the sorbent material. The CaO phase is accompanied by peaks corresponding to the mixed inert phase, $CaZrO_3$. After the reaction, only peaks characteristic of $CaCO_3$ appear in the diffractrogram of the spent sorbent together with the main peak of CaO at 37.4°, however with a very low intensity, indicating that the free CaO in the sorbent is almost completely converted to $CaCO_3$ which is in line with the

very high carbonation conversion of the material. After calcination of the sorbent, $CaCO_3$ completely decomposes to CaO again, as evidenced by the absence of $CaCO_3$ peaks in the diffractogram of the spent calcined sorbent.

In the case of the NiO/ZrO_2 OTM (Figure 3.14b), the presence of both NiO and the ZrO_2 support crystal phases is evident in the diffractogram of the fresh material. On the contrary, after the reduction/reforming/carbonation stage, NiO is almost completely reduced to metallic Ni which can generate the maximum amount of heat during its oxidation in the regeneration stage. This is also supported by the amount of the sorbent that was regenerated simultaneously with Ni reoxidation, which remained relative stable during the 20 SE-CL-SMR cycles.

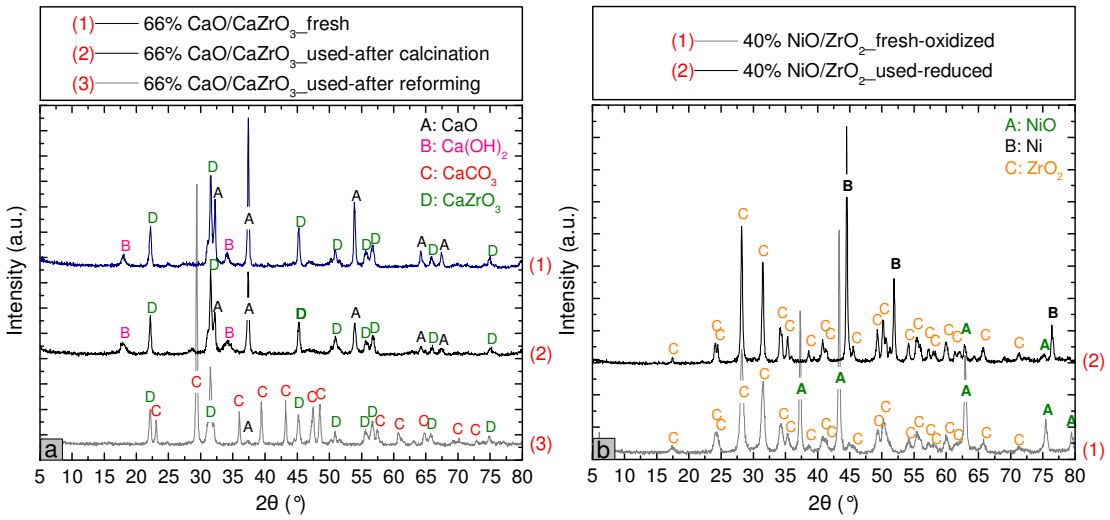

Figure 3.14: XRD patterns of fresh and used (after reforming stage and after calcination) 66% $CaO/CaZrO_3$ (a) and fresh and used 40% NiO/ZrO_2 (b).

4 Conclusions

This chapter presents the main conclusions reached during this dissertation. In this thesis, a novel reforming process for high purity H_2 production, namely Sorption Enhanced Chemical Looping Steam Methane Reforming, was investigated theoretically and experimentally. In this process, the methane reformer contains a Zr-promoted CaO-based sorbent ($CaO/CaZrO_3$) and a NiO-based oxygen transfer material (OTM)/reforming catalyst (NiO/ZrO_2). NiO is reduced by CH_4 and catalyzes the reforming reactions, while the sorbent captures in-situ the produced CO_2. The reaction can proceed under near autothermal conditions due to the heat released by the strongly exothermic carbonation reaction of the CO_2 sorbent, while the saturated sorbent is regenerated in a second step with the energy being provided by the exothermic Ni reoxidation, leading to an energetically well balanced process with overall minimum heat demands. The experiments as well as the thermodynamic analysis with Aspen software demonstrated the feasibility and the high potential of this novel process.

The preliminary evaluation of the CaO-based CO_2 sorbent under multiple sorption/desorption cycles in a thermogravimetric analyzer (TGA) and the NiO-based OTM/catalyst under conventional reforming reaction in a fixed bed flow unit indicated their suitability for the proposed process. $CaO/CaZrO_3$ exhibited very stable performance during cyclic operation with less than 14% loss of capacity and a high initial sorption capacity over 10 moles of CO_2/kg of sorbent. NiO/ZrO_2 OTM also showed a satisfactory activity in conventional SMR, with a high initial methane conversion of ~80% and a good stability during 10 h of reaction. The two materials, $CaO/CaZrO_3$ and NiO/ZrO_2 were further tested under sorption enhanced chemical looping reforming conditions in a bench scale flow unit at different operating conditions.

A range of temperatures (600, 650 and 700 °C) was examined to find the optimal operating temperature for the reforming reactor. During the reforming stage, in the pre-breakthrough period, high purity hydrogen over 88% is obtained at all temperatures, with values exceeding 95% at temperatures lower than 650°C. This is in good agreement with the findings of the thermodynamic analysis performed in the simulation

study, with only small deviation observed in the product concentrations compared to the ones dictated by equilibrium at the respective temperatures. Moreover, during the regeneration stage, when regeneration begins at higher temperatures (reforming temperatures of 650°C and 700°C), the heat generated by the highly exothermic Ni reoxidation increases the reactor's temperature to higher values compared to the case of 600°C, favoring the decarbonation of the saturated sorbent and resulting in larger amounts of sorbent regenerated simultaneously with Ni reoxidation. Furthermore at temperatures above 650°C, the sorption capacity of the sorbent gradually declines as the exothermic carbonation reaction is not favored at high temperatures, thereby reducing both hydrogen yield and purity and rendering the SE-CL-SMR process less attractive. As a result, the optimum reforming temperature in order to achieve both high H_2 purities and reduced overall requirements of the process approximates to be at 650 °C.

In addition to reforming temperature, a range of (S/C) ratios (2, 3 and 4) was tested to find the optimal for the reforming reactor. During the prebreakthrough period, the concentration of H_2 increases from ~92% to ~97% for an increase in S/C ratio from 2 to 4. An increase of S/C ratio shifts both WGS and reforming reactions to the product side, leading to higher hydrogen purity. For S/C ratios greater than 3 is not observed any substantial change in the efficiency of SE-CL-SMR process. However, a large excess of steam leads to higher energy demands for steam generation. Therefore, an intermediate S/C ratio close to 3 is preferred.

A crucial parameter in SE-CL-SMR process is NiO/CaO ratio, as the amount of Ni that is reoxidized during regeneration stage can determine the overall energy requirements of the process. A range of NiO/CaO ratios (0.2, 0.5 and 0.8) was examined to find the optimal one for the reforming reactor. At the prebreakthrough period, during the reforming stage, H_2 concentration slightly increases (95-97%) with increasing NiO/CaO ratio. According to the thermodynamics, as NiO/CaO ratio increases, more methane is oxidized and less is consumed by the reforming reaction. Even though a higher CH_4 conversion is achieved leading higher H_2 purity, this also results in a reduction of the overall H_2 yield of the process. During the regeneration stage, when NiO/CaO ratio was increased from 0.2 to 0.8, the temperature of the reactor reaches a maximum value of ~820°C and a respective increase of the duration of Ni reoxidation period to ~23 min. This results in covering in-situ almost 45% of the heat required for sorbent's regeneration. This value appear to be much lower compared to the simulation

study's results, where a similar high NiO/CaO ratio leads to almost complete cover of regenerator's thermal duty. This is however expected as thermodynamics doesn't take in to account the different rates of the two reactions (Ni oxidation and $CaCO_3$ calcination) and the heat losses occurring in more realistic conditions.

Last but not least, a range of residence times was examined by changing the inlet flow rate of CH_4 and maintain a constant S/C ratio of 3. Very high H_2 concentrations (~95 %) were achieved regardless the increase of spatial velocity in the experiments, demonstrating the high capture capacity of the sorbent, even when lower conduction times were applied, shifting the global reaction to values near to equilibrium. This a very important aspect, considering that the SE-CL-SMR process would mainly operate in a dual fluidized bed system with the materials circulating between the two reactors and the conduction times between the feed and the bed materials are relatively low.

The stability of the materials under cyclic SE-CL-SMR operation was tested for 20 reduction/reforming and regeneration cycles. Similar high H_2 concentrations were achieved during almost all the cycles, indicating that there was not significant deterioration in the performance of the two materials. Post-reaction characterization results were in line with the cyclic performance of the two solids, showing that the $CaO/CaZrO_3$ retains almost completely the surface area and porosity of the fresh material. On the other hand, a high decrease in the surface area of the OTM was observed after the reaction. Considering the high loading of NiO (40 wt %), the material is expected to be more prone to sintering. This sintering however did not deteriorate the catalytic performance in the experiment, probably due to the high amount of OTM employed. High amounts of OTM are required to provide heat for the sorbent regeneration; it is therefore anticipated that this would not affect the performance of the OTM in the actual process.

The simulation analysis and the experimental study over the synthetic CaO-based sorbent and NiO-based OTM/reforming catalyst demonstrated the feasibility and high potential of the combined SE-CL-SMR process. Despite the improvements achieved in the present thesis, there are still possible subsequent research challenges to be faced. Interesting aspects are the issues of the complexity of the process related to the handling of the physical mixture of the sorbent/OTM materials. In order to eliminate these issues the research efforts are directed to the development of bifunctional materials that combines both catalytic and absorption properties in a single pellet. The challenge however still remains in the reduced activity of such materials.

Bibliography

[1] P. P. Edwards, V. L. Kuznetsov, and W. I. F. David, "Hydrogen energy.," *Philos. Trans. A. Math. Phys. Eng. Sci.*, vol. 365, no. 1853, pp. 1043–1056, 2007.

[2] B. Johnston, M. C. Mayo, and A. Khare, "Hydrogen: the energy source for the 21st century," *Technovation*, vol. 25, no. 6, pp. 569–585, 2005.

[3] G. W. Crabtree, M. S. Dresselhaus, and M. V Buchanan, "The Hydrogen Economy," *Phys. Today*, no. December, pp. 39–45, 2004.

[4] G. Marbán and T. Valdés-Solís, "Towards the hydrogen economy?," *Int. J. Hydrog. Energ.*, vol. 32, pp. 1625–1637, 2007.

[5] N. Z. Muradov and T. N. Veziroğlu, "From hydrocarbon to hydrogen-carbon to hydrogen economy," *Int. J. Hydrogen Energy*, vol. 30, no. 3, pp. 225–237, 2005.

[6] T. I. Sigfusson, "Pathways to hydrogen as an energy carrier.," *Philos. Trans. A. Math. Phys. Eng. Sci.*, vol. 365, no. 1853, pp. 1025–1042, 2007.

[7] C. M. Kalamaras and A. M. Efstathiou, "Hydrogen Production Technologies : Current State and Future Developments," 2013, vol. 2013.

[8] M. V. Twigg, *Catalyst Handbook*, 2nd ed. London: Wolfe Publishing Ltd, 1989.

[9] J. D. Holladay, J. Hu, D. L. King, and Y. Wang, "An overview of hydrogen production technologies," *Catal. Today*, vol. 139, no. 4, pp. 244–260, 2009.

[10] B. Sorensen, *Hydrogen snd Fuel Cells*, 2nd ed. Academic Press, 2011.

[11] The Linde Group. Steam Reforming [Online]. Available at: http://www.linde-engineering.com/en/process_plants/hydrogen_and_synthesis_gas_plants/gas_generation/steam_reforming/index.html [Accessed: 2 December 2015]

[12] L. Barelli, G. Bidini, F. Gallorini, and S. Servili, "Hydrogen production through sorption-enhanced steam methane reforming and membrane technology: A review," *Energy*, vol. 33, no. 4. pp. 554–570, 2008.

[13] C. H. Bartholomew and R. J. Farrauto, *Methanol Synthesis*. 2006.

[14] K. Wawrzinek/ HDV / Nov. 21, Linde AG Linde Engineering Division 2007 /Industrial H2 Production & Technology.ppt

[15] O. Bičáková and P. Straka, "Production of hydrogen from renewable resources and its effectiveness," *Int. J. Hydrogen Energy*, vol. 37, no. 16, pp. 11563–11578, 2012.

[16] Roads2HyCom. On-site Hydrogen Generators from Hydrocarbons [Online]. Available at: http://www.ika.rwth-aachen.de/r2h/index.php/On-site_Hydrogen_Generators_from_Hydrocarbons.html [Accessed: 2 December 2015]

[17] Arno A. EVERS FAIR-PR. Production of Hydrogen without electricity from renewables [Online]. Available at: http://www.hydrogenambassadors.com/background/production-of-hydrogen-without-electricity-from-renewables.php [Accessed: 2 December 2015]

[18] M. F. Demirbas, "Hydrogen from Various Biomass Species via Pyrolysis and Steam Gasification Processes," *Energy Sources, Part A Recover. Util. Environ. Eff.*, vol. 28, no. 3, pp. 245–252, 2006.

[19] K. Tomishige and M. Asadullah, "Production of Syngas by Catalytic Gasification of Biomass at Low Temperature and Synthesis of Clean Transportation Fuels," vol. 2, no. 35, pp. 521–523, 2002.

[20] M. Ni, D. Y. C. Leung, M. K. H. Leung, K. H. Sumathy, "An overview of hydrogen production from biomass," *Fuel Processing Technology*, vol. 87, no.5, pp. 461 – 472, 2006.

[21] N. Muradov, "Emission-free fuel reformers for mobile and portable fuel cell applications," *J. Power Sources*, vol. 118, no. 1–2, pp. 320–324, 2003.

[22] a. Konieczny, K. Mondal, T. Wiltowski, and P. Dydo, "Catalyst development for thermocatalytic decomposition of methane to hydrogen," *Int. J. Hydrogen Energy*, vol. 33, no. 1, pp. 264–272, 2008.

[23] Agência Regional da Energia e Ambiente da Região Autónoma da Madeira. H2 A ECONOMIADO HIDROGÉNIO [Online]. Available at: http://www.aream.pt/download/brochuras/Brochura_hidrogenio.pdf [Accessed: 2 December 2015]

[24] J. Turner, G. Sverdrup, M. K. Mann et al., "Renewable hydrogen production," *Int. J. energy Res.*, vol. 32, no. 5, pp. 379–407, 2008.

[25] M. Ni, M. Leung, and D. Leung, "Technological development of hydrogen production by solid oxide electrolyzer cell (SOEC)," *Int. J. Hydrogen Energy*, vol. 33, no. 9, pp. 2337–2354, 2008.

[26] S. A. Gricoriev, V. I. Porembsky, and V. N. Fateev, "Pure hydrogen production by PEM electrolysis for hydrogen energy," *Int. J. Hydrogen Energy*, vol. 31, no. no. 2, pp. 171–175, 2006.

[27] D.P. Harrison, "Sorption-enhanced hydrogen production: a review," *Ind. Eng. Chem. Res.* 47 (2008) 6486–6501.

[28] M. Rydén and P. Ramos, "H_2 production with CO_2 capture by sorption enhanced chemical-looping reforming using NiO as oxygen carrier and CaO as CO_2 sorbent," *Fuel Process. Technol.*, vol. 96, pp. 27–36, 2012.

[29] H. R. Radfarnia and M. C. Iliuta, "Hydrogen production by sorption-enhanced steam methane reforming process using CaO-Zr/Ni bifunctional sorbent–catalyst," *Chem. Eng. Process. Process Intensif.*, vol. 86, pp. 96–103, 2014.

[30] A. M. Kierzkowska, R. Pacciani, and C. R. Müller, "CaO-based CO2 sorbents: From fundamentals to the development of new, highly effective materials," *ChemSusChem*, vol. 6, no. 7, pp. 1130–1148, 2013.

[31] J. Wang, L. Huang, R. Yang, and Z. Zhang, "Recent advances in solid sorbents for CO2 capture and new development trends," *Energy Environ. Sci.*, pp. 1–41, 2014.

[32] J. C. Abanades and D. Alvarez, "Conversion limits in the reaction of CO2 with lime," *Energy and Fuels*, vol. 17, no. 2, pp. 308–315, 2003.

[33] C. C. Dean, J. Blamey, N. H. Florin, M. J. Al-Jeboori, and P. S. Fennell, "The calcium looping cycle for CO2 capture from power generation, cement manufacture and hydrogen production," *Chem. Eng. Res. Des.*, vol. 89, no. 6, pp. 836–855, 2011.

[34] P. Xu, M. Xie, Z. Cheng, and Z. Zhou, "CO2 capture performance of CaO-based sorbents prepared by a sol-gel method," *Ind. Eng. Chem. Res.*, vol. 52, no. 34, pp. 12161–12169, 2013.

[35] V. Manovic and E. J. Anthony, "Lime-based sorbents for high-temperature co2 capture-a review of sorbent modification methods," *Int. J. Environ. Res. Public Health*, vol. 7, no. 8, pp. 3129–3140, 2010.

[36] A. Antzara, E. Heracleous, and A. a. Lemonidou, "Improving the stability of synthetic CaO-based CO2 sorbents by structural promoters," *Appl. Energy*, vol. 156, pp. 331–343, 2015.

[37] Z. Zhou, Y. Qi, M. Xie, Z. Cheng, and W. Yuan, "Synthesis of CaO-based sorbents through incorporation of alumina/aluminate and their CO2 capture performance," *Chem. Eng. Sci.*, vol. 74, pp. 172–180, 2012.

[38] L. F. de Diego, M. Ortiz, F. García-Labiano, J. Adánez, A. Abad, and P. Gayán, "Hydrogen production by chemical-looping reforming in a circulating fluidized bed reactor using Ni-based oxygen carriers," *J. Power Sources*, vol. 192, no. 1, pp. 27–34, 2009.

[39] K. S. Kang, C. H. Kim, K. K. Bae, W. C. Cho, S. H. Kim, and C. S. Park, "Oxygen-carrier selection and thermal analysis of the chemical-looping process for hydrogen production," *Int. J. Hydrogen Energy*, vol. 35, no. 22, pp. 12246–12254, 2010.

[40] M. Tang, L. Xu, and M. Fan, "Progress in oxygen carrier development of methane-based chemical-looping reforming: A review," *Appl. Energy*, vol. 151, pp. 143–156, 2015.

[41] H. Yang, Z. Xu, M. Fan, R. B. Slimane, A. E. Bland, and I. Wright, "Progress in carbon dioxide seperation and capture: A review," vol. 20, pp. 14–27, 2008.

[42] E. Karimi, H.R. Forutan, M. Saidi, M.R. Rahimpour, A. Shariati, Experimental study of chemical-looping reforming in a fixed-bed reactor: performance investigation of different oxygen carriers on Al2O3 and TiO2 support, Energy Fuel 28 (2014) 2811–2820

[43] a. Antzara, E. Heracleous, D. B. Bukur, and a. a. Lemonidou, "Thermodynamic analysis of hydrogen production via chemical looping steam methane reforming coupled with in situ CO2 capture," *Int. J. Greenh. Gas Control*, vol. 32, pp. 115–128, 2015.

[44] R.H. Perry, D.W. Green, J.O. Maloney, *Perry's chemical engineers' handbook,* McGraw-Hill, New York (1999).

[45] L. Silvester, A. Antzara, G. Boskovic, E. Heracleous, A. a. Lemonidou, and D. B. Bukur, "NiO supported on Al2O3 and ZrO2 oxygen carriers for chemical looping steam methane reforming," *Int. J. Hydrogen Energy*, vol. 40, no. 24, pp. 7490–7501, 2015.

[46] A. Antzara, E. Heracleous, and A. a. Lemonidou, "Development of CaO-based Mixed Oxides as Stable Sorbents for Post-Combustion CO2 Capture Via Carbonate Looping," *Energy Procedia*, vol. 63, no. November 2015, pp. 2160–2169, 2014.

[47] C. S. Martavaltzi and A. a. Lemonidou, "Hydrogen production via sorption enhanced reforming of methane: Development of a novel hybrid material-reforming catalyst and CO2 sorbent," *Chem. Eng. Sci.*, vol. 65, no. 14, pp. 4134–4140, 2010.

[48] B. L. Dutrow, C. M. Clark, X-ray Powder Diffraction (XRD) [Online]. Available at: http://serc.carleton.edu/research_education/geochemsheets/techniques/XRD.html [Accessed: 2 December 2015]

[49] M. Xie, Z. Zhou, Y. Qi, Z. Cheng, and W. Yuan, "Sorption-enhanced steam methane reforming by in situ CO2 capture on a CaO–Ca9Al6O18 sorbent," *Chem. Eng. J.*, vol. 207–208, pp. 142–150, 2012.

[50] D. K. Lee, I. H. Baek, and W. L. Yoon, “Modeling and simulation for the methane steam reforming enhanced by in situ CO2 removal utilizing the CaO carbonation for H2 production,” *Chem. Eng. Sci.*, vol. 59, no. 4, pp. 931–942, 2004.

[51] C. S. Martavaltzi, E. P. Pampaka, E. S. Korkakaki, and A. a. Lemonidou, “Hydrogen Production via Steam Reforming of Methane with Simultaneous CO_2 Capture over CaO–$Ca_{12}Al_{14}O_{33}$,” *Energy & Fuels*, vol. 24, no. 4, pp. 2589–2595, 2010.